

Spring 2012

# Mesoproterozoic Deposition, Regional Metamorphism and Deformation in North-Central New Mexico: Evidence from Metamorphic Monazite and Detrital Zircon Geochronology in the Picuris Mountains

Lily S. Pfeifer

*Bucknell University*, [lsp012@bucknell.edu](mailto:lsp012@bucknell.edu)

Follow this and additional works at: [https://digitalcommons.bucknell.edu/honors\\_theses](https://digitalcommons.bucknell.edu/honors_theses)



Part of the [Geology Commons](#)

---

## Recommended Citation

Pfeifer, Lily S., "Mesoproterozoic Deposition, Regional Metamorphism and Deformation in North-Central New Mexico: Evidence from Metamorphic Monazite and Detrital Zircon Geochronology in the Picuris Mountains" (2012). *Honors Theses*. 104.  
[https://digitalcommons.bucknell.edu/honors\\_theses/104](https://digitalcommons.bucknell.edu/honors_theses/104)

This Honors Thesis is brought to you for free and open access by the Student Theses at Bucknell Digital Commons. It has been accepted for inclusion in Honors Theses by an authorized administrator of Bucknell Digital Commons. For more information, please contact [dcadmin@bucknell.edu](mailto:dcadmin@bucknell.edu).

**MESOPROTEROZOIC DEPOSITION, REGIONAL METAMORPHISM AND  
DEFORMATION IN NORTH-CENTRAL NEW MEXICO: EVIDENCE FROM  
METAMORPHIC MONAZITE AND DETRITAL ZIRCON GEOCHRONOLOGY  
IN THE PICURIS MOUNTAINS**

By

**Lily S. Pfeifer**

A Thesis

Presented to the Honors Committee  
In Partial Fulfillment of the Requirements for the Degree of  
Bachelor of Science with Honors in Geology  
Bucknell University  
May, 2012

Approved:

  
\_\_\_\_\_

Christopher G. Daniel  
Thesis Advisor, Department of Geology, Bucknell University

  
\_\_\_\_\_

Jeffrey M. Trop  
Chair, Department of Geology, Bucknell University



**MESOPROTEROZOIC DEPOSITION, REGIONAL METAMORPHISM AND  
DEFORMATION IN NORTH-CENTRAL NEW MEXICO: EVIDENCE FROM  
METAMORPHIC MONAZITE AND DETRITAL ZIRCON GEOCHRONOLOGY  
IN THE PICURIS MOUNTAINS**

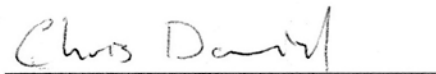
By

**Lily S. Pfeifer**

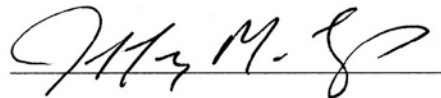
A Thesis

Presented to the Honors Committee  
In Partial Fulfillment of the Requirements for the Degree of  
Bachelor of Science with Honors in Geology  
Bucknell University  
May, 2012

Approved:



Christopher G. Daniel  
Thesis Advisor, Department of Geology, Bucknell University



Jeffrey M. Trop  
Chair, Department of Geology, Bucknell University

## ACKNOWLEDGMENTS

A special thank you goes to my thesis advisor, Dr. Chris Daniel, who has been a constant source of patient explanations and helpful guidance. His encouragement and reassurance throughout the duration of this research has allowed me to achieve all of my goals and beyond. I could not have been more fortunate to have the opportunity to work with him as my mentor. I would like to thank Dr. Mike Jercinovic, Dr. Mike Williams, and Dr. Julien Allaz for performing electron microprobe analyses at the University of Massachusetts, Amherst. Thank you to Dr. Jeff Trop and Dr. Bruce Idleman for assisting in zircon mount preparation, and to George Gehrels, Nicky Geisler, Mauricio Ibanez-Mejia, and Mark Pecha at the LaserChron at the University of Arizona for assistance conducting geochronologic analysis, as well as my fellow zircon zappers Erin Donaghy, Kyle Kissock, Tyler Szwarc, and Jeff Trop. The constant feedback and encouraging advice from my colleagues in senior program Jeremy Byler, Erin Donaghy, and Scott Lunde, advisors Dr. Jeff Trop and Dr. Ellen Herman, as well as other Bucknell Geology professors, played a crucial role in the creation of this thesis. I would like to thank my honor's thesis defense committee members, Dr. Chris Daniel, Dr. Jeff Trop, and Dr. Eric Tillman for the time they spent reading, revising, and discussing my thesis, and for administrating my defense this past April. Thanks to everyone who came to my first GSA presentation and to my honor's thesis defense; for helping to calm my nerves beforehand, and for celebrating together after. Thanks to Linda Mertz and Carilee Dill for the refreshing conversations we have shared, and for organizing trips and expenses. Thank

you to Brad Jordan for repairing the choking chipmunk crusher, and for always making time to teach me how to use equipment. I would like to especially thank my friends and family for their unconditional support. To my fellow O'Leary inhabitants, thank you for keeping me company late at night, and especially to Erin Donaghy for being my loyal partner through the growth of the thesis baby. I could not imagine doing any of this without Erin, the laughs we have shared, and of course our infamous Friday afternoon computer lab playlists! Thank you to all of my friends for dragging me out of the geology building now and then, and for being so understanding of my time commitments. To William, thank you for withstanding conversations about zircon and monazite over dinner, for being there to celebrate my accomplishments, and for converting my anxieties into positive energy. Finally, thank you to my wonderful mother and father Lisa Corbett and Richard Pfeifer, and my brother Chas, for listening to my rollercoaster of frustrations and triumphs, for providing resources I needed to reach my goals, for being so proud of my accomplishments, and for allowing me to have the opportunity to find my passions, and myself in the past four years at Bucknell.

Support for this project is funded by National Science Foundation grants EAR-0443387 to Jeff Trop and student grants from the Geological Society of America (to Lily Pfeifer), and the Bucknell University Program for Undergraduate Research (to Lily Pfeifer). The Bucknell University Department of Geology Marchand Fund and the Provost's Office provided financial support for travel and expenses for trips to Minneapolis for the national GSA conference, and to New Mexico and Arizona for sample collection and analyses.

**FORWARD**

This thesis was written by Lily Pfeifer except for the section entitled “*Detrital zircon geochronology methods*” adapted from Gehrels et al. (2008, 2006), and the section entitled “*U-Th-Pb chemical age dating methods*” adapted from Williams and Jercinovic (2007, 1999).

## TABLE OF CONTENTS

<b>ACKNOWLEDGEMENTS</b> .....	iv
<b>FORWARD</b> .....	vi
<b>TABLE OF CONTENTS</b> .....	vii
<b>LIST OF FIGURES</b> .....	ix
<b>LIST OF TABLES</b> .....	xi
<b>ABSTRACT</b> .....	1
<b>INTRODUCTION</b> .....	3
Significance of research.....	6
Regional geologic setting and lithostratigraphy of north-central NM.....	7
Tectonic history of north-central New Mexico.....	13
<b>METHODS</b> .....	17
Sample collection and preparation.....	17
Detrital zircon geochronology methods.....	20
U-Th-Pb chemical age dating.....	22
<b>RESULTS</b> .....	24
Quartzite petrology.....	24
Detrital zircon geochronology.....	24
<i>Zircon morphology</i> .....	24
<i>U-Pb detrital zircon ages</i> .....	27
Metamorphic monazite ages.....	35



<i>Compositional domains</i> .....	35
<i>U-Th-Pb chemical age data</i> .....	44
<b>DISCUSSION</b> .....	47
Detrital zircon ages.....	47
<i>Provenance of the Marquenas Fm</i> .....	52
Timing of metamorphism.....	59
Regional tectonic implications.....	61
<b>CONCLUSION</b> .....	63
<b>REFERENCES</b> .....	65

## LIST OF FIGURES

<b>Figure 1.</b>	Precambrian provinces in the southwest U.S. ....	4
<b>Figure 2.</b>	P-T loop diagram for north-central New Mexico.....	5
<b>Figure 3.</b>	Precambrian and plutonic exposures in central New Mexico.....	8
<b>Figure 4.</b>	Geologic map of the Picuris Mountains.....	9
<b>Figure 5.</b>	Photographs of Marquenas Formation quartzite and conglomerate.....	11
<b>Figure 6.</b>	Lithostratigraphic column of the Picuris Mountains.....	12
<b>Figure 7.</b>	Modern analogue for the Marquenas Formation.....	15
<b>Figure 8.</b>	Cross section through the Picuris Mountains.....	16
<b>Figure 9.</b>	Thin section light microscope photos.....	25
<b>Figure 10.</b>	Zircon mount light microscope images.....	26
<b>Figure 11.</b>	BSE images of concentric zoning in zircon grains.....	28
<b>Figure 12.</b>	BSE images of core and rim domains in zircon grains.....	29
<b>Figure 13.</b>	Age probability plot for all detrital samples.....	32
<b>Figure 14.</b>	U/Th ratios vs. U/Pb age plot.....	33
<b>Figure 15.</b>	Average age and concordia plot for igneous sample PIC-11.....	36
<b>Figure 16.</b>	Compositional maps of monazite grains in sample CD10-10.....	38
<b>Figure 17.</b>	Compositional maps of monazite grains in sample CD10-12.....	39

<b>Figure 18.</b>	Y and Ca Compositional maps with ages for sample CD10-10.....	41
<b>Figure 19.</b>	Y and Ca Compositional maps with ages for sample CD10-12.....	43
<b>Figure 20.</b>	Histogram of monazite ages for samples CD10-10 and CD10-12.....	45
<b>Figure 21.</b>	Minimum depositional age histograms of monazite domains.....	46
<b>Figure 22.</b>	Normalized probability plot of samples with previous data.....	49
<b>Figure 23.</b>	Maximum depositional age plot of Mesoproterozoic zircons.....	50
<b>Figure 24.</b>	Map of Picuris Mountains with paleocurrent data.....	53
<b>Figure 25.</b>	Regional map of the southwest U.S. showing ca. 1.4 Ga plutons.....	54
<b>Figure 26.</b>	Map of northern NM with ca. 1.4 Ga plutonic sources.....	55

**LIST OF TABLES**

<b>Table 1.</b>	Sample locations and names.....	18
<b>Table 2.</b>	Summary of detrital ages for sandstone samples from the Picuris.....	30
<b>Table 3.</b>	Composition and age of monazite core and rim domains.....	37
<b>Table 4.</b>	Results of K-S statistical test.....	51

## ABSTRACT

Detrital zircon and metamorphic monazite ages from the Picuris Mountains, north central New Mexico, were used to confirm the depositional age of the Marquenas Formation, to document the depositional age of the Vadito Group, and to constrain the timing of metamorphism and deformation in the region.

Detrital zircon  $^{207}\text{Pb}/^{206}\text{Pb}$  ages were obtained with the LA-MC-ICPMS from quartzites collected from the type locality of the Marquenas Formation exposed at Cerro de las Marquenas, and from the lower Vadito Group in the southern and eastern Picuris Mountains. The Marquenas Formation sample yields 113 concordant ages including a Mesoproterozoic age population with four grains ca. 1470 Ga, a broad Paleoproterozoic age peak at 1695 Ma, and minor Archean age populations. Data confirm recent findings of Mesoproterozoic detrital zircons reported by Jones et al. (2011), and show that the Marquenas Formation is the youngest lithostratigraphic unit in the Picuris Mountains. Paleoproterozoic and Archean detrital grains in the Marquenas Formation are likely derived from local recycled Vadito Group rocks and ca. 1.75 Ga plutonic complexes, and ca. 1.46 Ga detrital zircons were most likely derived from exposed Mesoproterozoic plutons south of the Picuris. Ninety-five concordant grains from each of two Vadito Group quartzites yield relatively identical unimodal Paleoproterozoic age distributions, with peaks at 1713-1707 Ma. Eastern exposures of quartzite mapped as Marquenas Formation yield detrital zircon age patterns and metamorphic mineral assemblages that are nearly identical to the Vadito Group. On this basis, I tentatively assigned the easternmost

quartzite to the Vadito Group. Zircon grains in all samples show low U/Th ratios, well-developed concentric zoning, and no evidence of metamorphic overgrowth events, consistent with an igneous origin. North-directed paleocurrent indicators, such as tangential crossbeds (Soegaard & Eriksson, 1986) and other primary sedimentary structures, are preserved in the Marquenas Formation quartzite. Together with pebble-to-boulder metaconglomerates in the Marquenas, these observations suggest that this formation was deposited in a braided alluvial plain environment in response to syn-tectonic uplift to the south of the Picuris Mountains.

Metamorphic monazite from two Vadito Group quartzite samples were analyzed with an electron microprobe (EMP). Elemental compositional variation with respect to Th and Y define core and rim domains in monazite grains, and show lower concentrations of Th (1.46-1.52 wt%) and Y (0.67 wt%) in the cores, and higher concentrations of Th (1.98 wt%) and Y (1.06 wt%) in the rims. Results show that Mesoproterozoic core and rim ages from five grains overlap within uncertainty, ranging from 1395-1469 Ma with an average age of 1444 Ma. This 1.44 Ga average age is the dominant timing of metamorphic monazite growth in the region, and represents the timing of metamorphism experienced by the region. An older 1630 Ma core observed in sample CD10-12 may be interpreted as a result of low temperature metamorphism in lower Vadito Group rocks due to heat from ca. 1.65 Ga granitic intrusions. Core ages ca. 1.5 Ga are likely due to a mixing age of two different age domains during analyses. Confirmed sedimentation at 1.48-1.45 Ga and documented mid-crustal regional

metamorphism in northern New Mexico ca. 1.44-1.40 are likely associated with a Mesoproterozoic orogenic event.

## **INTRODUCTION**

Precambrian metamorphic rocks in New Mexico record the tectonic evolution of Laurentia. Evidence of ca. 1.48-1.40 Ga plutonism, metamorphism, deformation, and sedimentation is recognized in north-central New Mexico but the tectonic setting is not well understood (Jones et al., 2011; Daniel & Pyle, 2006; Kirby et al., 1995; Nyman, 1994). There is debate over whether to classify this 1.48-1.40 Ga activity as the result of anorogenic, localized heating and deformation that followed 1.65 Ga tectonism, or instead, as a regional, “orogenic” mountain building event.

Widespread crustal deformation and metamorphism in the southwestern United States occurred when volcanic island arcs were accreted onto the southern margin of Laurentia during the Yavapai (1.75-1.72 Ga) and Mazatzal (1.65-1.60 Ga) orogenies (Fig. 1; Karlstrom & Bowring, 1988; Karlstrom et al., 2004). Earlier studies in the region propose a polymetamorphic model in which all crustal folding, faulting, and metamorphism in New Mexico occurred during the Mazatzal and Yavapai orogenies between 1.75-1.60 Ga (Williams et al., 1999; Bauer, 1993). Between about 1.60-1.50 Ga Paleoproterozoic rocks were interpreted to cool and then remain in the middle crust. Intruding plutons ca. 1.48-1.35 Ga reheated the middle crust, and caused more localized deformation and metamorphism associated with an intracratonic tectonic event in

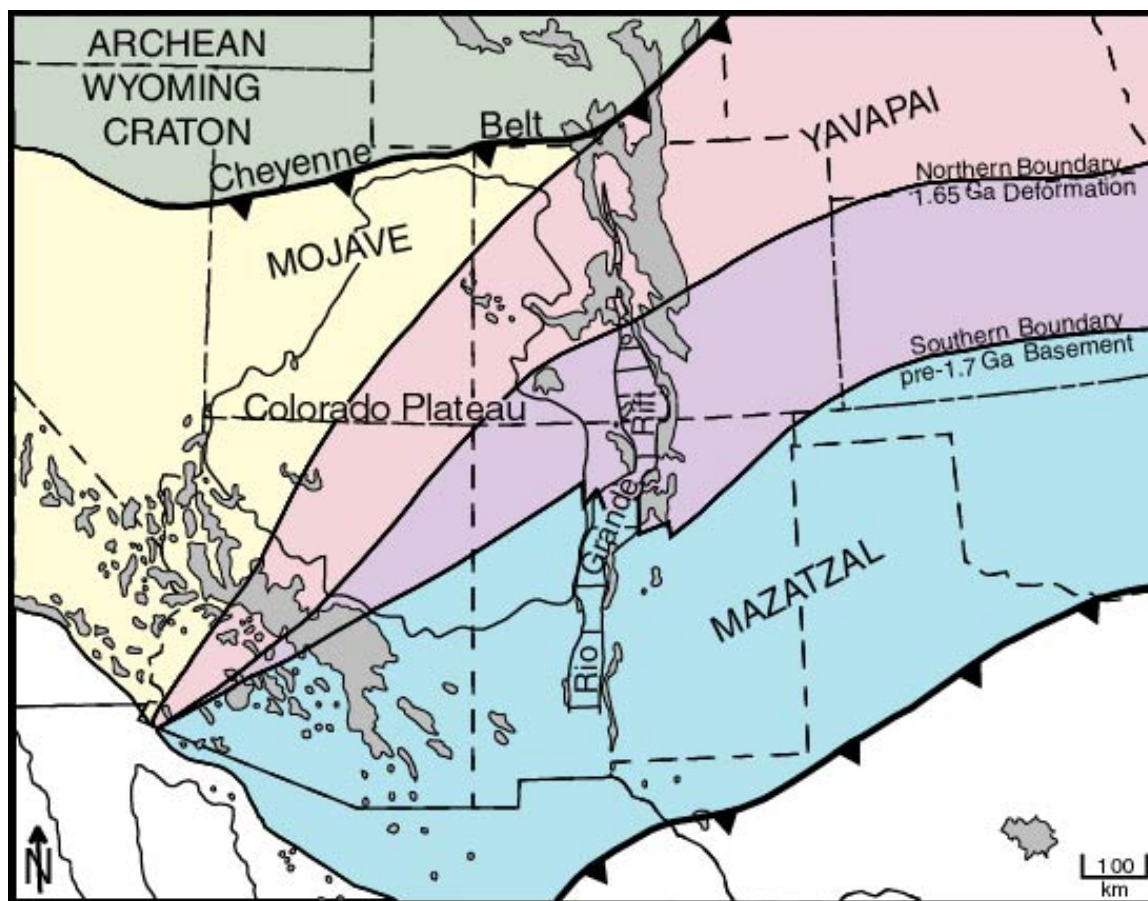


**Figure 1.** Map showing Precambrian-age provinces in the southwest U.S. (simplified from Karlstrom and Daniel, 1993) which record the history of continental growth ca. 1.8-1.6 Ga. Archean craton (>2 Ga) represents the core of the continent. The Yavapai Province was accreted to the edge of the continent 1.75-1.70 Ga, and the Mazatzal Province collided ca. 1.65-1.60 Ga.



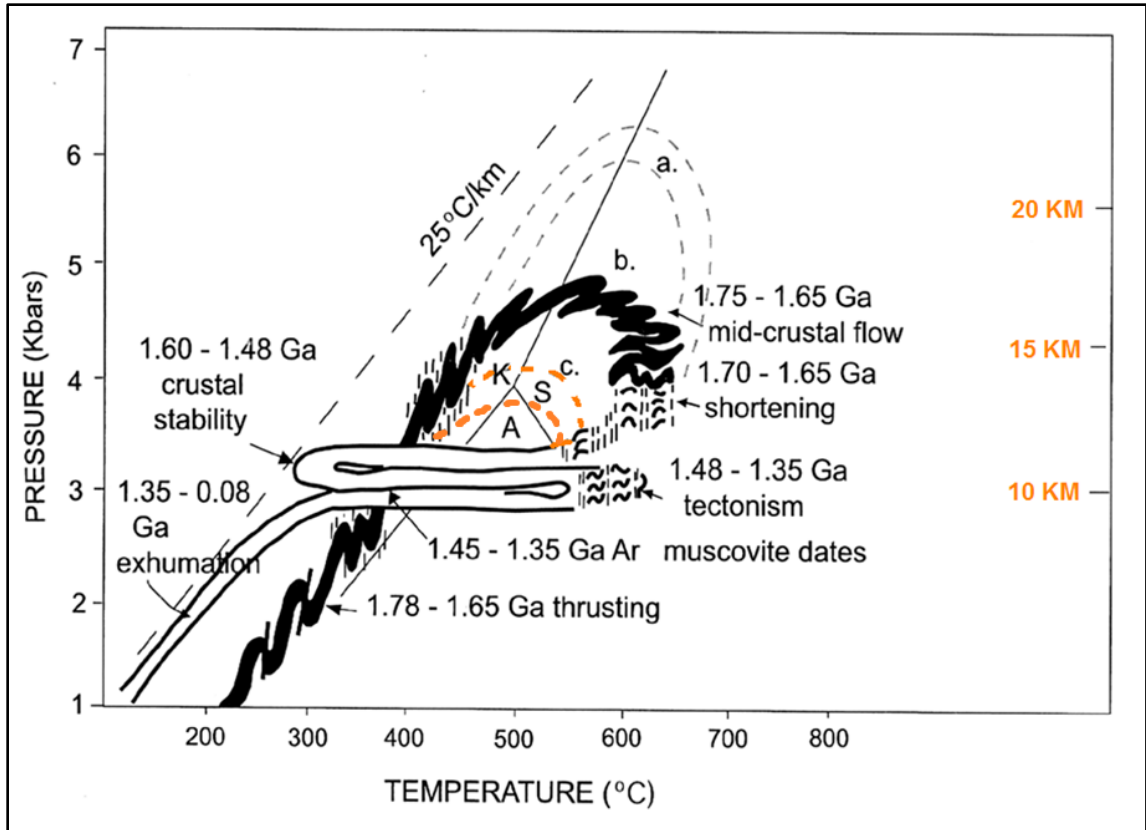


**Figure 2.** Polymetamorphic P-T paths from Karlstrom et al. (2004) proposed for three different mountain ranges in northern New Mexico: the Taos Mountains (a), Rincon Mountains (b), and path c (orange) is for the Picuris Mountains. P-T paths show Yavapai/Mazatzal (1.75-1.65 Ga) heating, compression, and deformation, followed by cooling and a residence time in the middle crust of about 200 Ma. The white P-T path represents isobaric reheating and minor tectonism around 1.4 Ga. Orange numbers defined on the second vertical axis represent the depths to which the rocks were buried (in km). Labels K, A, S and the lines in the center of the diagram define the kyanite, andalusite, sillimanite triple point which is around 500 °C and 4 kbar pressure.

northern New Mexico (Fig. 2; Karlstrom et al., 2004, 1997; Shaw et al., 2005; Read et al., 1999; and Williams et al., 1999; Karlstrom & Humphreys, 1998).

Other workers have proposed that pervasive 1.48-1.35 Ga granitic plutonism is the result of a significant mountain building event that occurred in response to compression at the plate margin to the distal south (Karlstrom & Dallmeyer, 1997; Kirby et al., 1995; Nyman et al., 1994). Daniel & Pyle (2006) documented regional metamorphism and deformation at 1.45-1.44 Ga by dating metamorphic monazite from the northern Picuris, and proposed that crustal thickening, plutonism, regional metamorphism and deformation may represent a single orogenic cycle in the southwestern U.S. ca. 1.45 Ga. More recently, Jones et al. (2011) found 1.48-1.46 Ga detrital zircons from the Marquenas Formation in the southern Picuris Mountains, likely sourced from nearby eroding granitic plutons to the south. These are the first reported detrital zircons of this age in the southwest U.S. and provide direct evidence for deposition of sediment sometime after 1.46 Ga.

### **Significance of research**

My research examines quartzite from the Picuris Mountains in an attempt to constrain the maximum and minimum depositional age of the Marquenas Formation, to document the timing of metamorphism and deformation in the region, and ultimately, to better understand the Mesoproterozoic tectonic setting of southern Laurentia. In this study, new U-Pb detrital zircon ( $ZrSiO_4$ ) geochronologic data and U-Th-Pb metamorphic monazite ([LREE]  $PO_4$ ) chemical age data are integrated with existing detrital zircon and

monazite geochronological data from the Picuris to constrain the timing of deposition, regional metamorphism, and deformation in northern New Mexico.

The youngest detrital zircon age population represents the maximum depositional age of the Marquenas Formation and metamorphic monazite ages record the timing of metamorphism in the region. Due to confusion about the age of the Marquenas Formation, previous work offers inconclusive and often contradictory evidence regarding its position within the regional lithostratigraphic framework, as well as its provenance and tectonic significance. New detrital zircon ages, when coupled with paleocurrent data (Soegaard & Eriksson, 1986, 1985; Barrett & Kirschner, 1979), depositional environment interpretations (Mawer et al., 1990; Soegaard & Eriksson, 1986), and ages of regional plutonic sources (Karlstrom et al., 2004) provide information that is critical to understand the tectonic history of northern New Mexico.

### **Regional geologic setting and lithostratigraphy of north-central New Mexico**

Precambrian rocks across northern New Mexico (1.8-1.45 Ga) are divided into four main lithostratigraphic sequences that are exposed in several Precambrian basement uplifts including the Tusas, Picuris, Truchas, Rio Mora, and Rincon Mountains (Fig. 3). The Picuris Mountains (Fig. 4) are a key location to observe stratigraphic and deformational relationships between the different rock formations. As noted by Bauer (1993), “Any stratigraphic, structural or tectonic model must succeed in the Picuris Range if it is to be applicable to northern New Mexico.” From oldest to youngest these lithostratigraphic divisions include: (1) metamorphosed mafic metavolcanic sequences

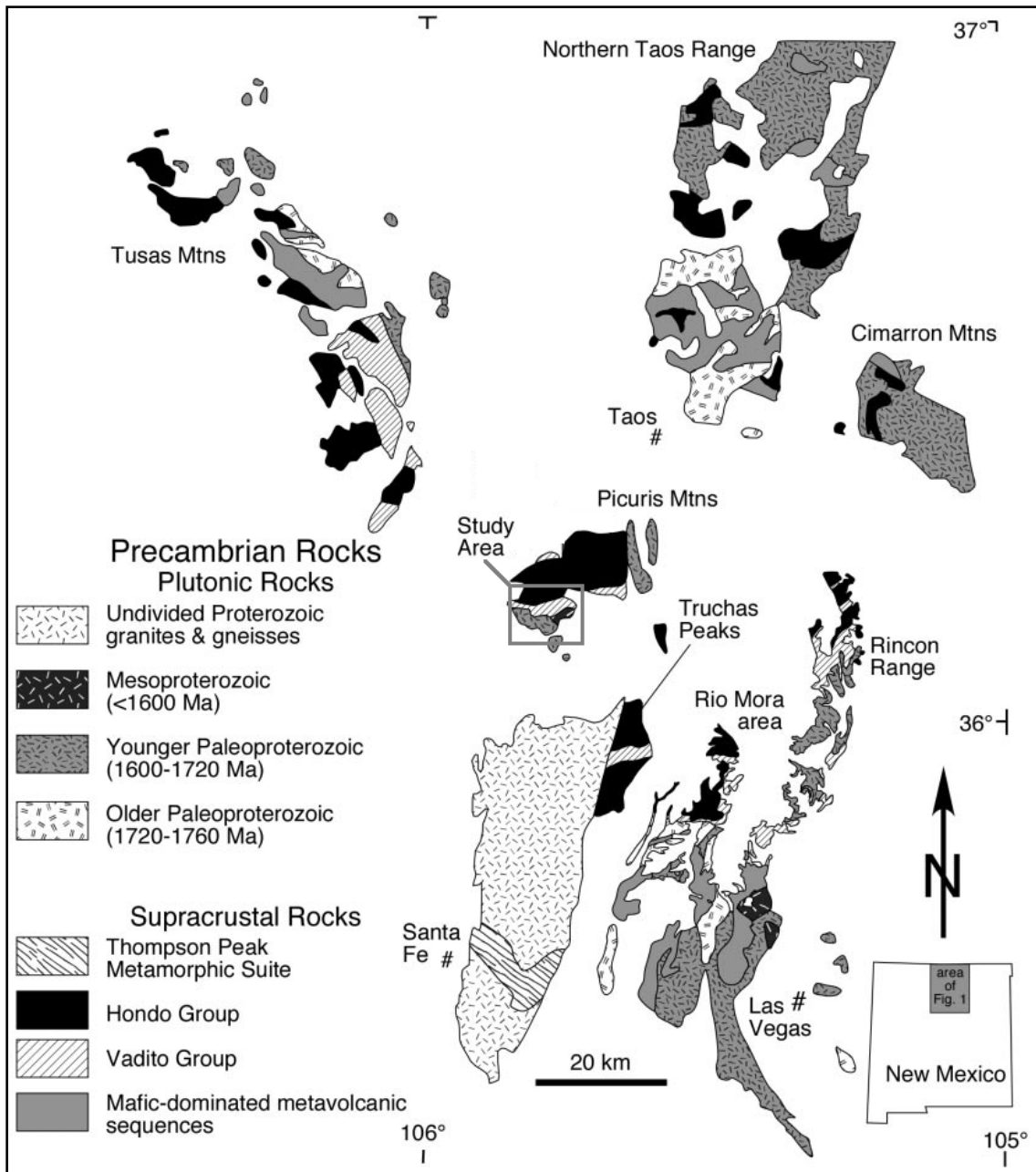


**Figure 3.** Simplified geologic map showing the distribution of Proterozoic rocks in north-central New Mexico (adapted from Daniel and Pyle, 2006). Study area in the Picuris Mountains is indicated with the grey box.

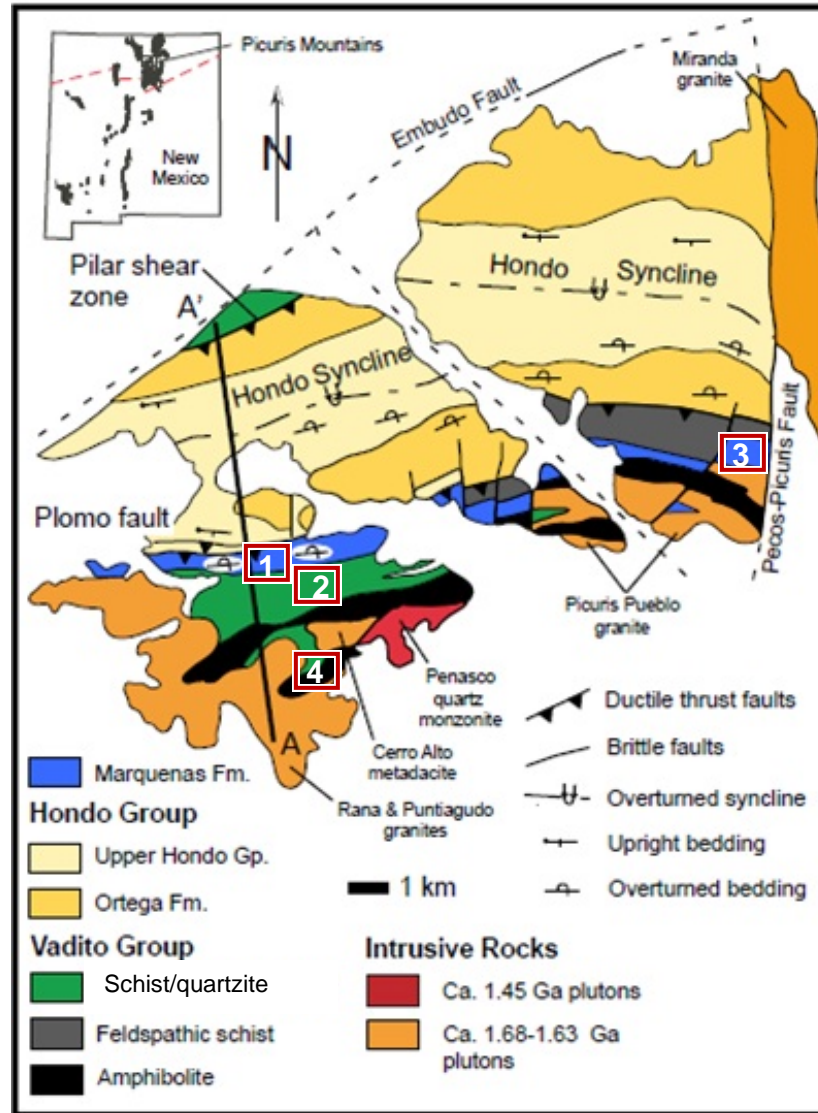


**Figure 4.** Simplified geologic map showing Proterozoic rocks in the Picuris Mountains (adapted from Jones et al., 2011). All formations are folded, faulted, sheared, and metamorphosed. Note large-scale Hondo Syncline. Sample locations are indicated by red boxes include: (1) type locality Cerro de las Marquenas quartzite south of the Plomo fault (LP11-03), (2) Vadito Group quartzite adjacent to the Pecos-Picuris Fault (mapped here as Marquenas Fm.), (3) Vadito Group quartzite in the southern Picuris (PIC-7), and (4) Picuris Pueblo granite intrusion south of Vadito quartzite (PIC-11).

(1.77 Ga-1.72 Ga) including the Moppin, Pecos, and Gold Hill Complexes (2) the felsic and mafic metavolcanic and metasedimentary 1.71-1.70 Ga Vadito Group, (3) a massive, 2050 meter-thick sequence of metamorphosed quartzite, minor quartz-pebble conglomerate, schist, and slate known as the Hondo Group (1.70-1.69 Ga), and (4) the Marquenas Formation, a 500 meter-thick sequence of metamorphosed pebble to boulder conglomerate and quartzite (Fig. 5; Bauer & Williams, 1989; Soegaard & Eriksson, 1986). Soegaard & Eriksson (1986) combined both the older mafic metavolcanic complexes and the Vadito Group together, but these two groups were later separated based on discrepancies in ages between underlying, mafic-dominant metavolcanics >1.71 Ga and 1.71-1.70 Ga Vadito Group rocks (Williams, 1982). Major and minor trace element analyses also show compositional differences between the two units (Bauer, 1989). In the Picuris, the Hondo Group consists of the basal Ortega Formation (850-1000 meters thick), overlain by the Rinconada, Pilar and Piedre Lumbre Formations (Soegaard & Eriksson, 1986). The type locality Marquenas Formation is exposed in the southern Picuris, and until recently, it was considered part of the older 1.70 Ga Vadito Group (Bauer et al. 1994; Williams, 1991; Bauer & Williams, 1989). Unlike the Vadito and Hondo Groups, the Marquenas contains both 1.70-1.60 Ga detrital zircons and 1.48-1.46 Ga detrital zircons. For this reason, the Marquenas was reinterpreted to unconformably overlie the Vadito and Hondo Groups (Fig. 6; Jones et al., 2011).

Regional metamorphic conditions in the southern Picuris are estimated to be 600 °C at 3.0-4.0 kbar in andalusite-cordierite schist immediately south of the Marquenas Formation (Williams et al., 1999) and about 525-540 °C at 4.0- 4.2 kbar in the northern

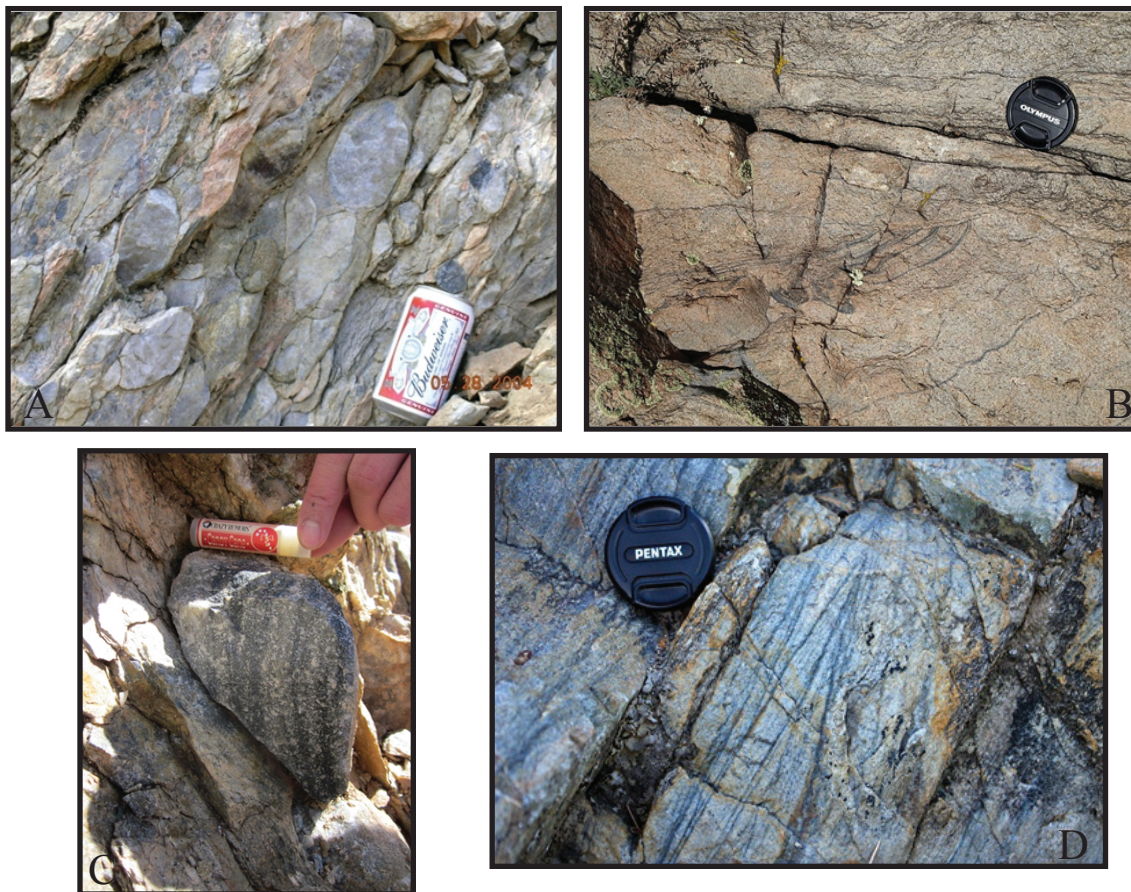


**Figure 5.** Photos of representative lithologies from the Marquenás Formation type locality (LP11-03) include (A) pebble to boulder metaconglomerate with dominantly quartzite clasts and minor rhyolite clasts and (B) thick quartzite with north-facing tangential crossbeds. (C) Minor cross-bedded quartzite clasts in the basal metaconglomerate units of the Marquenás. Image D was taken of Vadito Group crossbedded quartzite sample CD10-10 from the eastern Picuris.

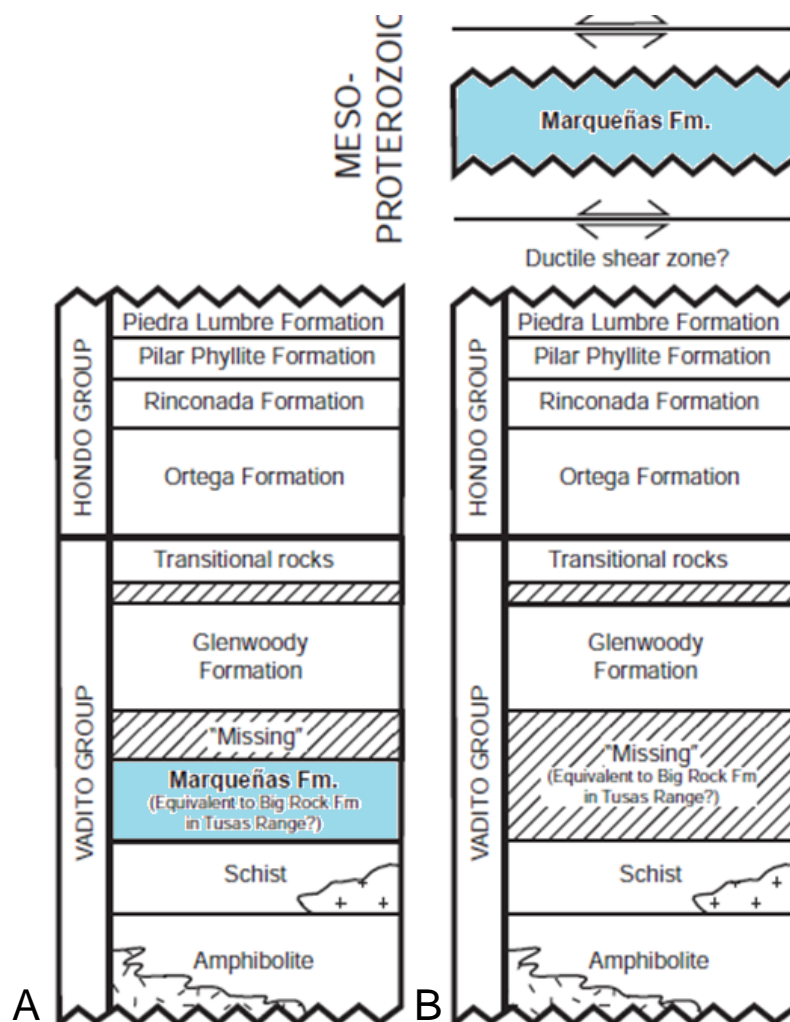


**Figure 6.** Schematic lithostratigraphic column for the Picuris Mountains. (A) The Marqueñas Formation was previously interpreted to be part of the Paleoproterozoic Vadito Group (Bauer & Williams, 1989; Bauer, 1993). (B) Marqueñas Formation is determined to be Mesoproterozoic in age and is placed unconformably over Hondo Group rocks (~250 Ma younger) in the Picuris stratigraphic column. Between the Marqueñas and Hondo Group is a shear zone defined by flattened clasts in the basal conglomerate of the Marqueñas and other shear sense indicators. This contact is observed locally in the Picuris.



Picuris (Daniel & Pyle, 2006). Ages of intrusive granitic plutons in the southern Picuris Range fall between 1680-1450 Ma (Bauer, 1988; D.A. Bell, 1986). Although the entire succession was metamorphosed at the amphibolite facies, primary sedimentary structures and lithologies preserve evidence of provenance, the depositional processes that operated, and environments that existed during deposition of each formation.

### **Tectonic history of north-central New Mexico**

Regional U/Pb age data (Stacey & Hedlund, 1983) support that the Vadito Group and mafic juvenile volcanic crust developed across the southwest U.S. 1.75-1.72 Ga during the Yavapai Orogeny in a back-arc tectonic setting (Soegaard & Eriksson, 1986). Granitic plutons extensively intruded metamorphic basement complexes and Vadito Group rocks, and caused thermal expansion and uplift of the crust. These units include the Gold Hill complex (1.77 Ga), the Moppin complex (>1.75 Ga) intruded by 1.69-1.65 Ga plutons, and the Pecos complex (1.72 Ga) (Bauer, 1989). Subsequent cooling allowed for subsidence and a period of prolonged tectonic stability, which accommodated deposition of thick, shallow marine shelf sediments of the Hondo Group around 1.70-1.69 Ga (Soegaard & Eriksson, 1986, 1985). Abundant primary sedimentary structures in the basal Ortega Formation of the Hondo Group include herringbone cross stratification, symmetrical ripples, and tangential crossbeds which suggest a northern source. Schists and slates of the Rinconada Formation represent an upward transition from quartz arenite to interbedded quartzite and mudstone, interpreted as a deltaic environment (Soegaard & Eriksson, 1989, 1986). Conglomerates and thick, interbedded quartzites of the Marquenas

Formation suggest that it was deposited on a braided alluvial fan (Fig. 7; modern analogue). The basal, pebble to boulder conglomerate contains subrounded to rounded, dominantly gray quartzite clasts and minor rhyolite and amphibolite clasts (Fig. 5bc). Dominantly north-dipping tangential crossbeds in quartzite beds (Fig. 5a) are consistent with a southern source (Soegaard & Eriksson, 1986) opposite that of the Hondo Group.

Soegaard & Eriksson (1986) used evidence of south-to-north paleocurrent indicators and clast composition to propose that the Marquenas was sourced from the Vadito Group basement rock and Ortega (Hondo) Group shelf sediments, and that deposition of the Marquenas was in response to uplift of the Vadito-Hondo cratonic margin to the south. They interpreted the Marquenas Formation as the youngest unit in the Picuris, and speculated that the destruction of the cratonic margin that sourced the Marquenas may have resulted from subduction-related orogenesis. Mawer et al. (1990) disagreed, and proposed that the Marquenas was not derived from erosion and re-deposition of the Hondo Group. Based on textural and mineralogical observations, clast population analysis, and structural interpretation, they suggested that the Marquenas Formation was stratigraphically in the upper part of the Vadito Group, related by a gradational (non-tectonic) contact. They observed that only 50-60% of clasts were fine-grained quartzite and contained no aluminum silicate minerals, in contrast to Hondo Group quartzite which is coarse-grained and rich in aluminum silicates (Grambling & Williams, 1985). Mawer et al. (1990) also report that Vadito quartzite and calc-silicate lithologies are mineralogically identical to clasts in the Marquenas. Detrital zircon results

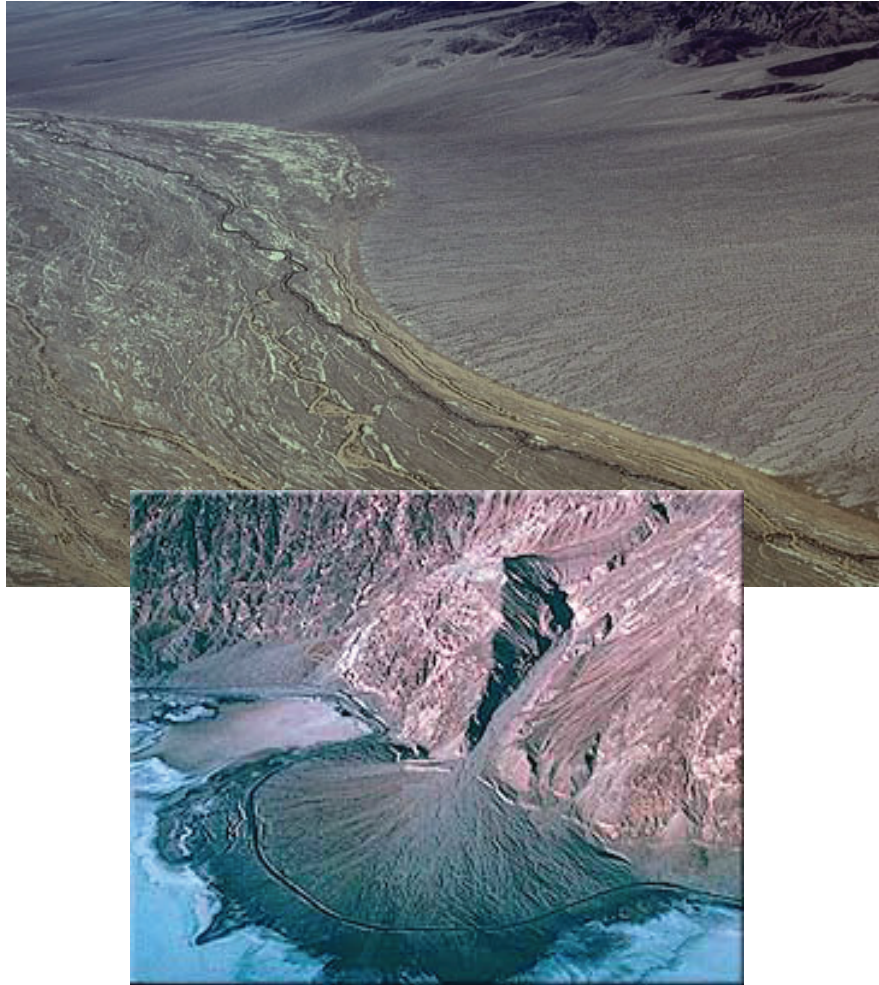


**Figure 7.** Modern analogue of the depositional environment of the Marquenas Formation. These photos show pictures of the Badwater Fan in Death Valley National Park. Braided streams operate on an alluvial fan at the base of a mountain, prograding out into the basin (Badwater Basin). Material is poorly sorted and contains pebble to boulder sized cobbles on the proximal part of the fan. In more distal parts of the fan (top photo) sediment is mostly composed of sand-sized detritus, similar to what composed the quartzite lithologies of the Marquenas Formation before metamorphism.

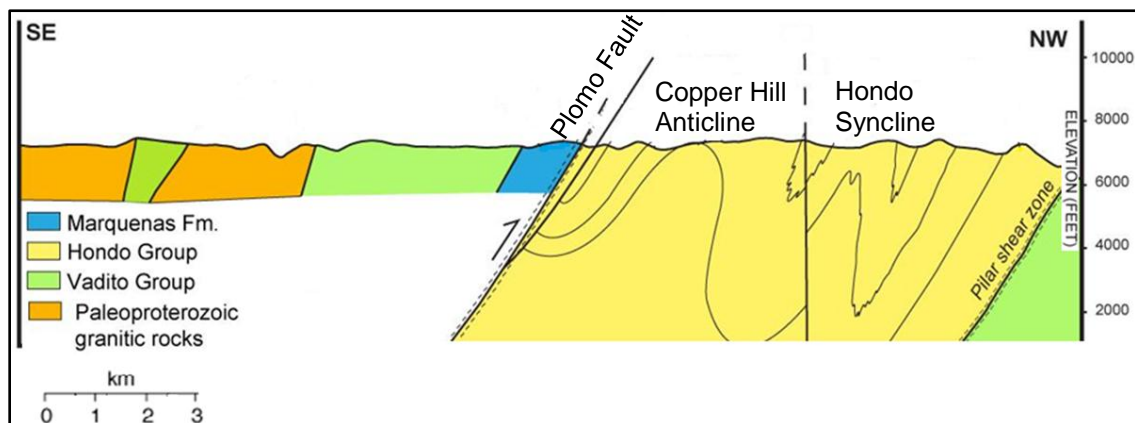


**Figure 8.** Northwest-southeast cross section through the Picuris Range (from Jones et al., 2011). Note km-scale folds of Hondo Syncline and Copper Hill anticline. Marquenas Formation (blue) sits between the Vadito Group and the Hondo Group south of the Plomo thrust fault.

confirm that the Marquenas Formation is the youngest unit in the Picuris, and is faulted against the Hondo Group (Fig. 8).

## **METHODS**

Detrital zircon methods are provided by the University of Arizona LaserChron Center (Gehrels et al., 2008, 2006) and methods of electron microprobe analyses are described by the University of Massachusetts, Amherst EMP facility (Williams & Jercinovic, 2005, 1999).

### **Sample collection and preparation**

Two oriented quartzite samples were collected from the upper Marquenas Formation in the southern Picuris Range, north-central New Mexico (Fig. 4). Dr. Chris Daniel and Dr. Jamey Jones previously collected samples from the upper Marquenas Formation and adjacent Vadito Group rocks that supplement my sample collection, and are included in analyses (Table 1). Spatially oriented thin sections were cut from each sample for light microscope imaging to determine the size and abundance of zircon grains, and how they relate to the deformational fabrics of the quartzite. Light microscope images of zircon grain mounts were assembled into a detailed photo mosaic that allowed for efficient location of various grains during analysis with the microprobe. Rock chips were cut, mounted in epoxy, and polished for two 15-minute cycles using 15 $\mu$ m, 9 $\mu$ m, and 3 $\mu$ m diamond suspension. Mounts were examined on the scanning electron microscope and energy dispersive x-ray spectroscopy (SEM/EDS) to determine the

**Table 1.** Locations of samples included in this study.

Number	Lat, long	Orientation	Formation	Lithologies	Analysis
LP11-03	N 36° 12.394', W 105° 48.345'	098, 80 S	Upper Marquenas	Quartzite	Detrital zircon
CD10-10	N 36° 13.951', W 105° 39.308'	300, 25 S	Vadito	Quartzite	Detrital zircon & Monazite
CD10-12	N 36° 12.388', W 105° 45.702'	065, 85 S	Vadito	Quartzite	Monazite
PIC-7	N 36° 11.283', W 105° 47.102'	N/A	Vadito	Conglom.	Detrital zircon
PIC-11	N 36° 13.535', W 105° 39.219'	unoriented	Vadito	Granite intrusion	Detrital zircon

\*Additional quartzite samples discussed in this study were collected and analyzed for detrital zircon by Jones et al. (2011) including PIC-2 (Middle Marquenas Fm.), PIC-3 (Upper Marquenas Fm.) PIC-5 (Upper Rinconada Fm.), PIC-1 (Ortega Fm), and PIC-4 (Upper Ortega Fm).

presence of monazite grains in each sample. The SEM allows for observation and identification of minerals within a sample. Back scatter electron (BSE) images were taken on the SEM for all monazite grains and about 55 zircon grains in each of the three samples in order to observe compositional zoning, inclusions, and the crystal morphology of the grains. Based on the abundance and size monazite grains present, four thin section samples were sent to the University of Massachusetts for mapping in preparation for U-Th-Pb chemical age dating with the electron microprobe. Thin section mapping of metamorphic monazite must be complete well in advance of analysis to allow time to study the microstructure and distribution of monazite in context of full section compositional maps. Care was taken to select metamorphic monazite grains that are large enough, cover all of the observed compositional variation, and to avoid grains that are damaged with cracks or inclusions.

For zircon separation, three quartzite samples and a granite sample were broken down into fist-size chunks, crushed into coarse grains with a jaw crusher, and pulverized into sand-size grains with several, increasingly narrow runs through the disc mill. Samples were sieved between runs to avoid pulverizing zircon grains into sizes smaller than sand or silt-size grains, which are too small for analyses. Zircon grains were extracted at the Lehigh University laboratory by traditional methods of heavy mineral separation involving a Wilfley table, density separation with methylene iodide, and a Frantz magnetic separator to eliminate strongly magnetic particles. All zircons were retained in the final heavy mineral fraction. Each sample yielded about 300 zircon grains that were incorporated into a 1" diameter epoxy mount with standard zircon grains (R33

and SL). These mounts were sanded and polished to a depth of ~20 microns, exposing the interior of the grains, cleaned, and imaged prior to isotopic analysis.

### **Detrital zircon geochronology methods**

Zircon ( $\text{ZrSiO}_4$ ) is used for geochronological analysis because of its near universal presence in crustal rocks, its negligible concentration of Pb, and its resistance to alteration of the U-Th-Pb isotopic system (Gehrels et al., 2008; Harley and Kelly, 2007). I conducted isotopic analyses in June, 2011 and again in December, 2011 by laser ablation multi-collector inductively coupled plasma mass spectrometry (LA-MC-ICPMS) at the Arizona LaserChron Center.

Care was taken to avoid cracks and inclusions in zircon grains during analysis, but otherwise ~110 zircon grains from each detrital sample (LP11-03, PIC-7, and CD10-10) and ~30 grains from the igneous sample (PIC-11) were selected randomly for each analysis with the laser. Ablation of zircon grains was done with the New Wave UP193HE Excimer laser using a spot diameter of 30  $\mu\text{m}$  and a pit depth of 5-15  $\mu\text{m}$ . About twenty rim areas of grains in each sample were analyzed with a smaller spot diameter of 10  $\mu\text{m}$ . The ablated material from the zircon grain is transported in helium gas to the plasma source of a Nu HR ICPMS which measures U, Th, and Pb isotopes simultaneously. A standard Sri Lanka zircon (SL) with a known age of  $563.5 \pm 3.2$  Ma was measured after every fifth analysis to correct for any error. Ratios of  $^{206}\text{Pb}/^{238}\text{U}$  and  $^{207}\text{Pb}/^{235}\text{Pb}$  were calculated with the Isoplot software program (Ludwig, 2008) and resulted in a measurement error of ~1-2% (at  $2\sigma$  level). There is also a  $2\sigma$  uncertainty for  $^{206}\text{Pb}/^{207}\text{Pb}$



ages for grains that are >1.0 Ga, which applies to all of my samples. Concentrations of U and Th are calibrated relative to this standard as well (contains ~518 ppm of U and 68 ppm Th). For  $^{206}\text{Pb}/^{207}\text{Pb}$  and  $^{206}\text{Pb}/^{238}\text{U}$  ages the uncertainty resulting from these calibration corrections is generally 1-2%. Data that are >20% discordant or >5% reverse discordant (by comparison of  $^{206}\text{Pb}/^{238}\text{U}$  and  $^{206}\text{Pb}/^{207}\text{Pb}$  ages) are eliminated and the remaining ages are plotted on Pb/U concordia diagrams and relative age-probability plots using the Isoplot program in Excel (Ludwig, 2008). It is unlikely that three or more grains will experience lead loss or gain and yield the same age, age clusters with  $\geq 3$  grains is considered significant (Gehrels et al., 2008).

The Kolmogorov-Smirnoff (K-S) statistical test was used to assess the similarity of the detrital zircon age distributions and determine what the statistical difference is between samples (Dickinson and Gehrels, 2009). I also included detrital zircon data from previously published studies that analyzed other Proterozoic quartzite formations exposed in the Picuris to possibly compare the samples I analyzed to ages of adjacent units. The test mathematically determines the probability (P) that the two age distributions were drawn from the same population. If the P value is >0.05, there is a 95% confidence that two populations are not statistically different. The higher the P value, the more likely it is that the two age distributions were drawn from the same population, or source. Unfortunately, the test cannot confirm that any two age populations are the same, only the probability that they are not (Gehrels, 2008; Guynn, 2006).

## **U-Th-Pb Chemical age dating methods**

Monazite ([LREE] PO<sub>4</sub>), a light rare earth element-bearing phosphate mineral is a common accessory phase in metamorphic rocks. It is used for U-Th-Pb chemical age dating because it is rich in U and Th, radiogenic Pb accumulates quickly in its structure and it can tolerate high radiation without experiencing lead loss. Electron microprobe analyses are a non-destructive, efficient, in-situ dating technique that has a very small spatial resolution of only 1-3  $\mu\text{m}$  (Montel, 1996), allowing discrete measurements to be recorded on the core and rim of the grains. These type of analyses permit observation of growth/overgrowth events in the monazite grain through several geologic events, and provide a two dimensional image of age distribution that helps to unravel complex polyphase metamorphic histories (Williams & Jercinovic, 2007, 1999; Montel, 1996). A preliminary assumption holds that the amount of non-radiogenic lead is negligible (<1 ppm), and no partial lead loss has occurred in the grain. Precision for this method is best in Precambrian, high pressure rocks with monazite that contains a significant amount of lead (>2000 ppm) and shows age differences of at least 100 Ma. For Th-rich Precambrian monazite, any individual age has a high uncertainty of  $\pm 40$  Ma, but for an entire age population the error is less than 10 Ma.

U-Th-Pb chemical age analyses were conducted with the electron microprobe (EMP) in September, 2011 by Mike Williams, Mike Jercinovic, and other individuals at the University of Massachusetts, Amherst EMP facility. Analytical strategies are dependent on compositional x-ray maps of selected monazite grains which were

constructed to characterize the distribution and variation in concentrations of Ca, Na, Th, U and Y in each compositional domain. Differential zoning from the core to the rim of the monazite grain may likely suggest distinct generations of mineral growth and consumption. Mapping requires an accelerating voltage of 25 keV, Faraday cup current (200-250 nA), pixel size 0.2-2.0 mm and dwell times of 50-100 ms/pixel. Element maps were collected and processed with the program *NIH Image*. Major element and trace element analyses [Th, U, Y, Ca, Nd] are repeated in each major domain until an age error has been achieved, or the area available for analysis is depleted. Five to ten analyses are required to achieve a stable  $2\sigma$  uncertainty on trace element analysis, and at least three grains must overlap within error to qualify for a reasonable confidence level (Williams et al., 2007). Before each monazite analysis, 1-3 standard grains with a well-known age are dated to minimize error (Jercinovic & Williams, 2005; Gratz, 1998; Montel, 1996). A useful estimate of random measurement errors from multiple different domains is the standard deviation of the mean. Results, including the mean and  $2\sigma$  error, are reported by a normal probability distribution with an area unity. This displays the array of ages and their distributions within a grain, and help to understand how levels of U, Th, and Pb change through metamorphic, deformational, and fluid circulation events.

## RESULTS

### Quartzite petrology

Light microscope and SEM imaging of samples LP11-03 and CD10-10 reveal the presence of large, relatively undeformed, equant quartz grains with straight grain boundaries, uniform extinction and minor sub-grain development (Fig. 9). Straight, equigranular to polygonal, triple-grain boundaries of recrystallized quartz crystals suggest metamorphism at medium temperatures (400-500°C; Passchier & Trouw, 2005). Smaller, recrystallized quartz grains (50-100 µm) have straight, triple grain boundaries. Rutile, ilmenite, and other iron oxides define oxide-rich compositional layering. In CD10-10 large, high relief zircon grains are present in oxide rich layers (~100µm). Muscovite and minor weathered biotite are also present, and in sample CD10-10 microcline composes 10-15% of the mineral composition. Myrmekite textures exhibit an intergrowth of quartz and potassium feldspar. No shear sense is obvious.

### Detrital zircon geochronology

#### *Zircon morphology*

Light microscope images show that grains in sample CD10-10 are light yellow in color and grains in LP11-03 are clear (Fig. 10). Mesoproterozoic grains (ca. 1.4 Ga) in sample LP11-03 are more rounded than older grains, consistent with a higher degree of transport. Paleoproterozoic zircon morphologies are equant to prismatic and generally

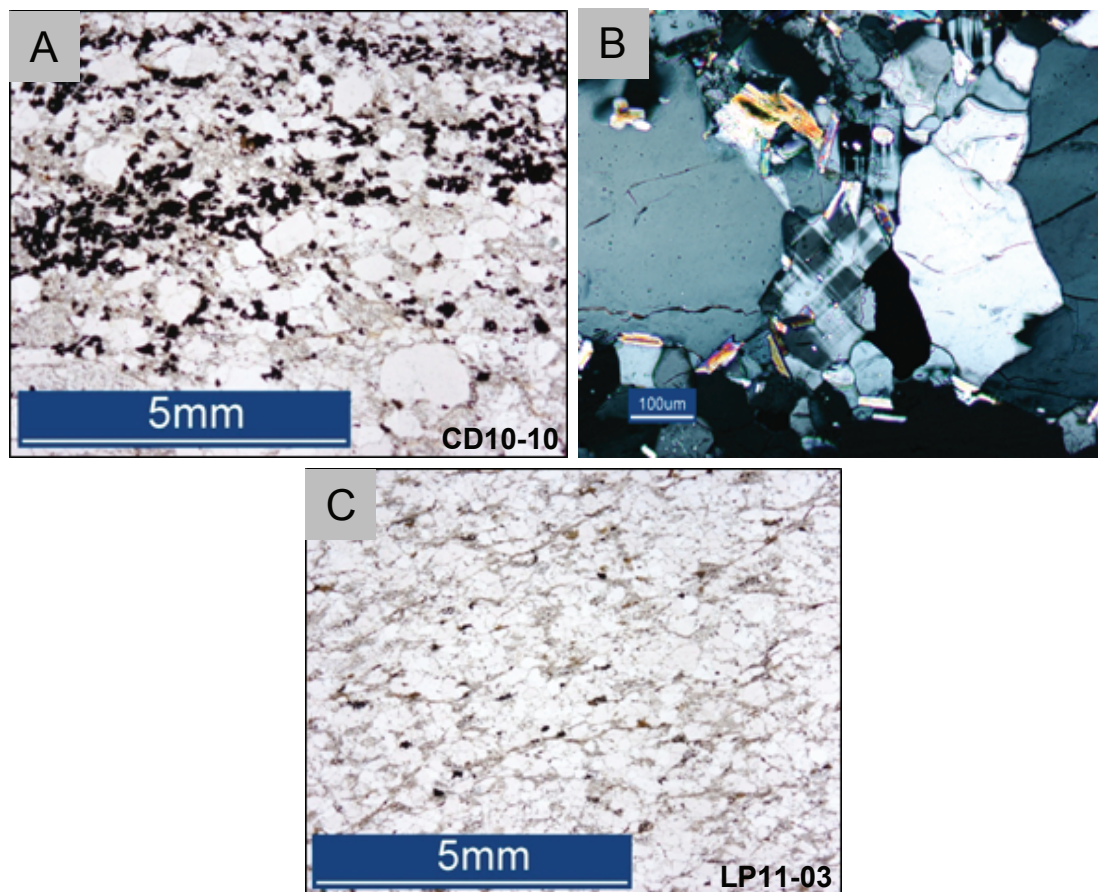


**Figure 9.** Light microscope images of thin sections from CD10-10 (A and B) and LP11-03 (C). Note large, equant quartz grains (A) and microcline crystals (B) in CD10-10. Smaller, recrystallized quartz grains have straight, triple grain boundaries. Muscovite, minor biotite, and iron oxides are also present in both samples.

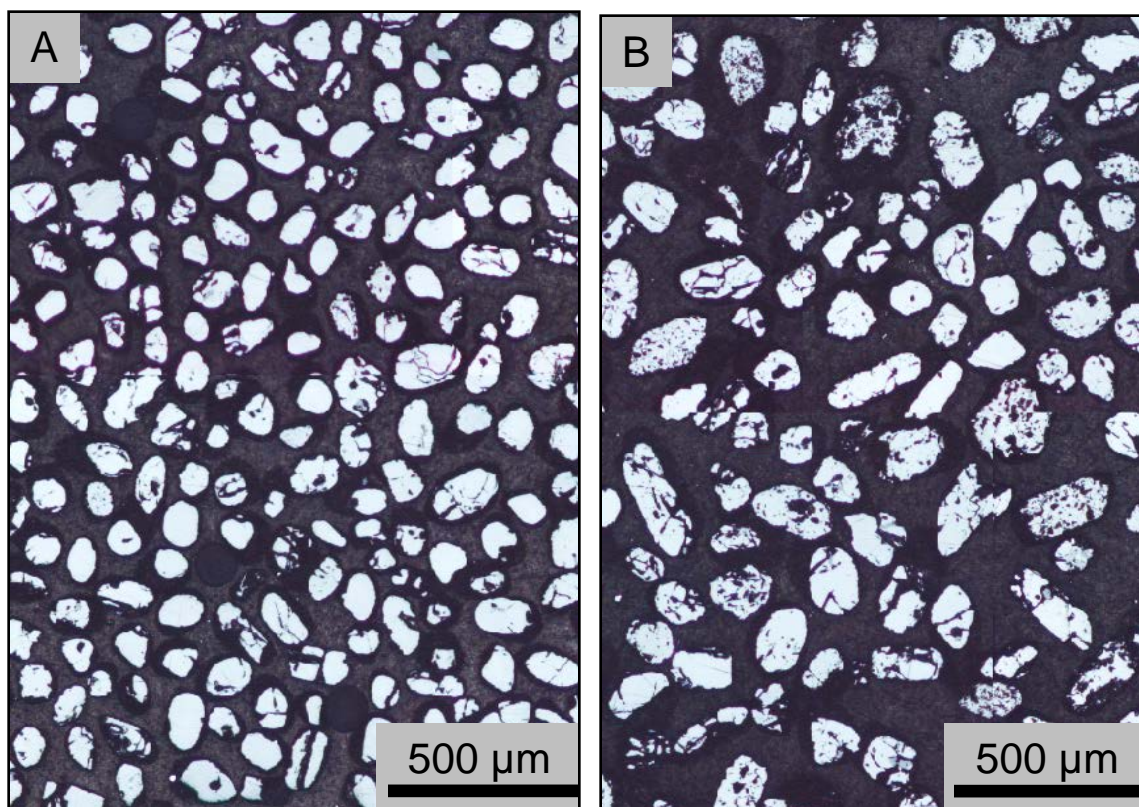


**Figure 10.** Light microscope images of detrital zircon grain mounts of sample LP11-03 (A) and sample CD10-10 (B). Most grains are subhedral to rounded, and are cracked and fractured.

more yellow than grains in sample LP11-03. BSE images of all detrital grain mounts analyzed show fractured, euhedral to subhedral grains of a uniform size distribution, with well-developed concentric zoning (Fig. 11), and distinct core and rim domains (Fig. 12).

#### *U-Pb detrital zircon ages*

Four samples were analyzed to provide a more complete record of the depositional history and provenance of the stratigraphic succession in the Picuris Mountains. Samples were collected from the middle Marquenas Formation quartzite (LP11-03), the Vadito Group quartzite (CD10-10), the Vadito Group conglomerate (PIC-7), and the Vadito Group granite (PIC-11). Approximate sample locations are shown in Figure 4 and GPS coordinates for each sample are found in Table 1. Analytical age data are summarized in Table 2. Data that are >20% discordant or >5% reverse discordant are eliminated. Age-probability diagrams and concordia plots for each sample show individual spot ages plotted as normalized distributions based on reported age and uncertainty (Fig. 13; Ludwig, 2003). Data-point error ellipses in concordia plots are shown for the 68.3% confidence interval ( $1\sigma$ ).

Zircon that grow from metamorphic fluids commonly show U/Th ratios > 10 but igneous zircon plot U/Th ratios < 10 (Gehrels et al., 2008). U/Th ratios for all samples are plotted in Figure 14, and more than 99.6% of analyzed zircons maintain a U/Th ratio < 10, with especially low ratios observed in Mesoproterozoic grains. Rim domains show homogeneously Paleoproterozoic ages (1800-1700 Ma), and one 1475 Ma Mesoproterozoic rim which matches its 1465 Ma age core (Fig. 12). All core and rim

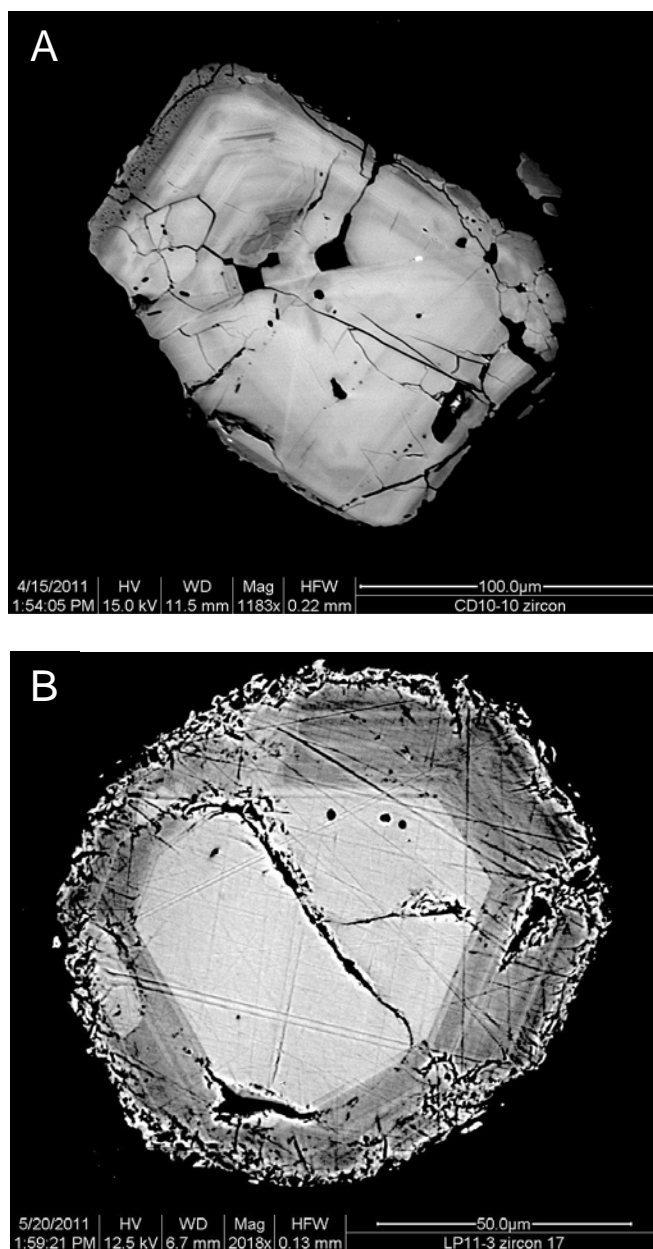


**Figure 11.** Back scatter electron image of a detrital zircon grain from sample CD10-10 (A) and sample LP11-03 (B) with well-defined concentric zoning. Note also in photo B the roundness of the Mesoproterozoic grain. The fracture is confined to the core of the grain and concentric zoning is consistent with an igneous origin.



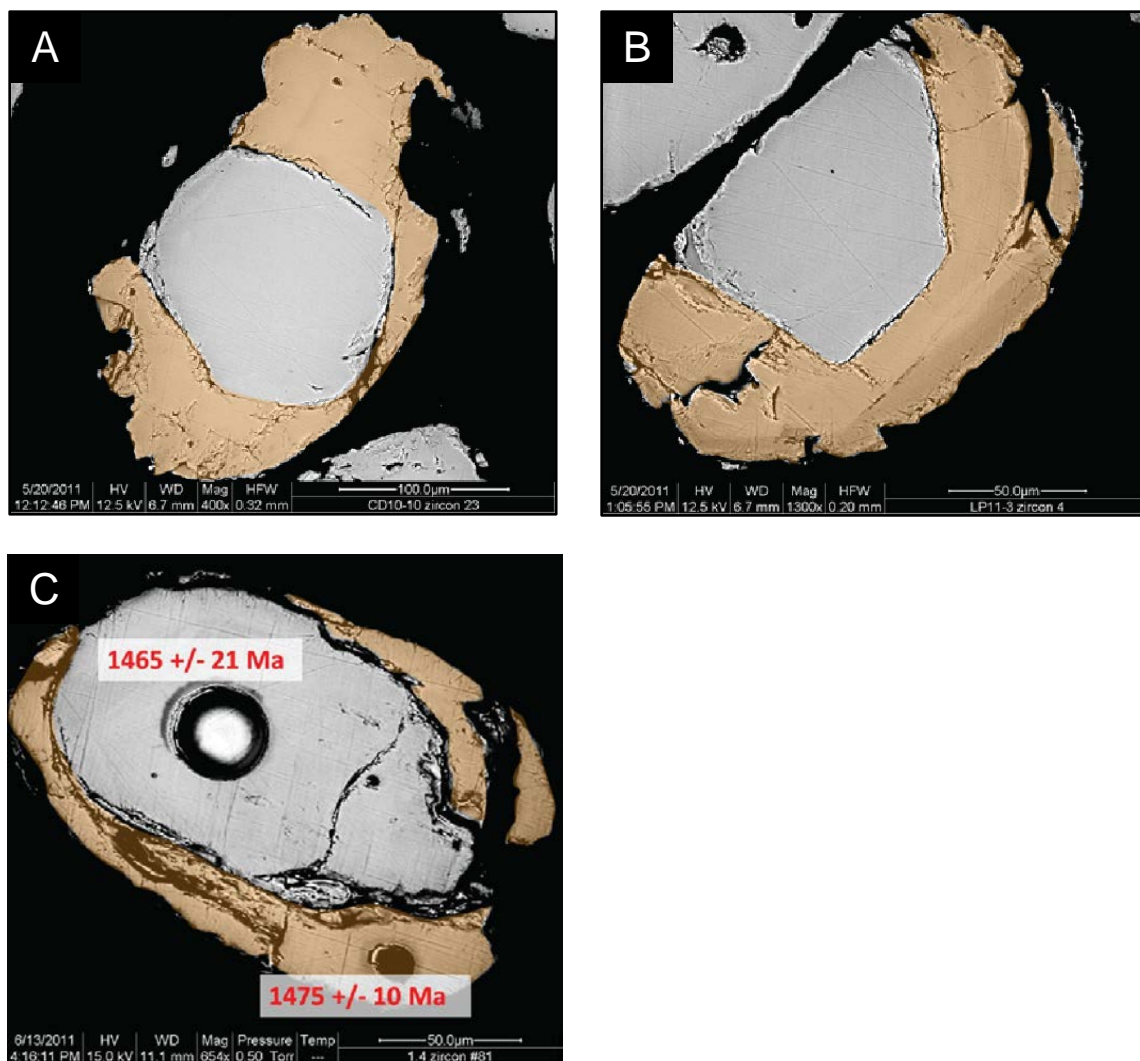


**Figure 12.** False color BSE images of detrital zircon grains from sample CD10-10 (A) and sample LP11-03 (B and C). Distinct domains are shown in gray (core) and orange (rim). Note the roundness of the cores in grain A and C. Pits are apparent in image C showing points of analyses. Core age  $1465 \pm 21$  Ma with  $30\mu\text{m}$  spot size and rim age  $1475 \pm 10$  Ma with  $10\mu\text{m}$  spot size.

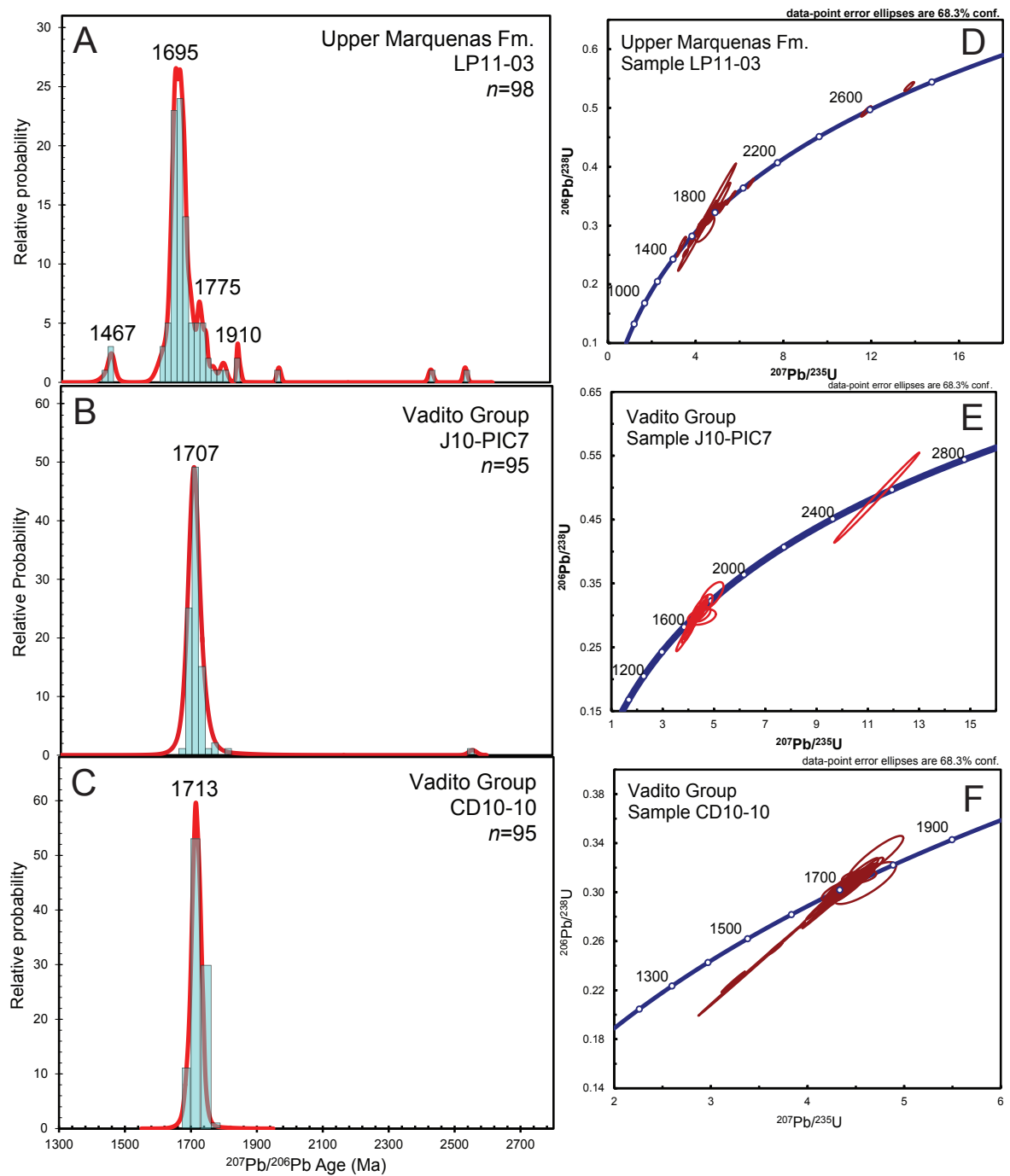
**Table 2.** Summary of detrital ages for sandstone samples from the Picuris.

<i>Sample LP11-03 (n=98)</i>	# grains	pop %	range	main peak	other peaks
Mesoproterozoic (1.4-1.6)	4	4%	1459-1475		1467
Paleoproterozoic (1.6-2.5)	92	92%	1651-2055	1697	1775, 1910, 2050, 2700
Archean (2.5-3.5)	2	2%	2584-2704		
<i>Sample PIC-7 (n=95)</i>	# grains	pop %	range	main peak	other peaks
Mesoproterozoic (1.4-1.6)	0	0%			
Paleoproterozoic (1.6-2.5)	94	99%	1677-1803	1707	
Archean (2.5-3.5)	1	1%			
<i>Sample CD10-10 (n=95)</i>	# grains	pop %	range	main peak	other peaks
Mesoproterozoic (1.4-1.6)	0	0%			
Paleoproterozoic (1.6-2.5)	95	100%	1686-1738	1713	
Archean (2.5-3.5)	0	0%			

\*Note that “n”= number of samples analyzed. See figure 4 for sample locations.

**Figure 13.** Relative age probability plot showing distribution of U-Pb ages and concordia diagrams for all analyzed samples. Heights of peaks are statistically significant, and the “n” value defines the number of zircon grains analyzed. (A) Quartzite sample LP11-03 from the upper Marquenas Fm. contains 98 concordant detrital zircon grains with a 1467 Ma Mesoproterozoic age population. Archean grain with age  $3529.8 \pm 3.6$  Ma is excluded in concordia plot. (B) Metaconglomerate sample PIC-7 from the Vadito Group contains 95 concordant detrital zircon grains yielding a unimodal broad 1707 Ma Paleoproterozoic age population peak. (C) Quartzite sample CD10-10 from the Vadito Group contains 95 concordant detrital zircon grains with unimodal broad 1713 Ma Paleoproterozoic age population peak.

Figure 13.



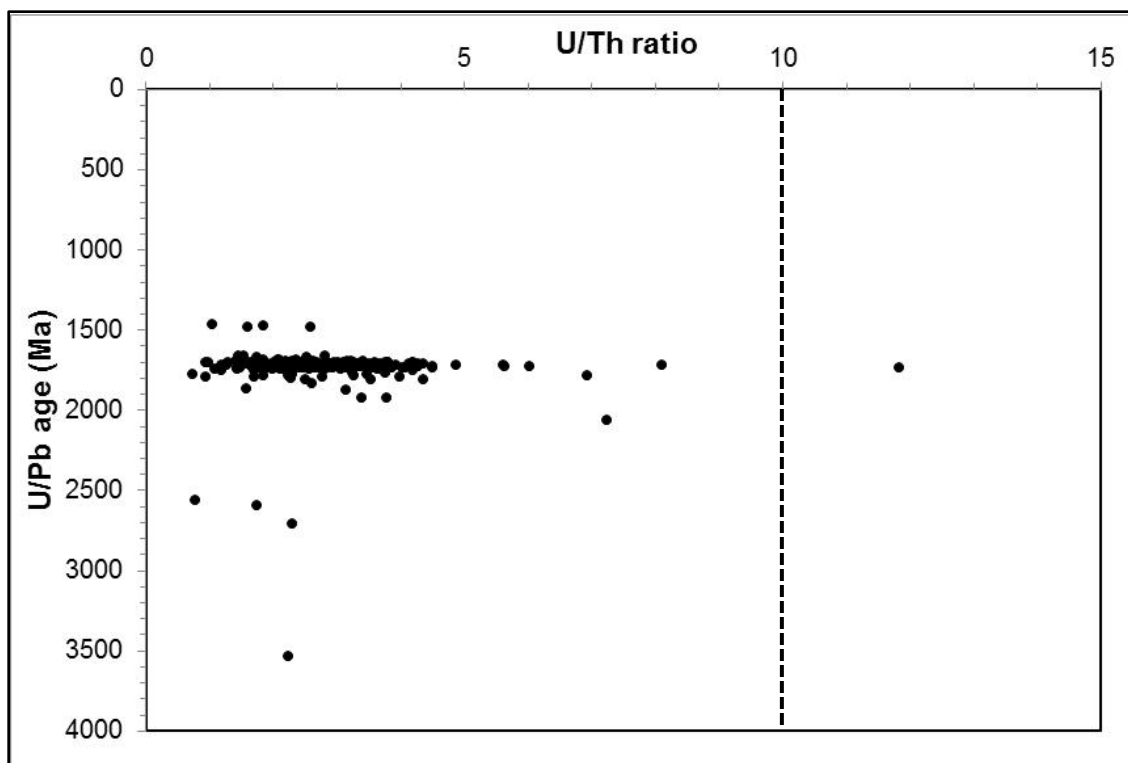


**Figure 14.** U/Th vs. U/Pb age of spot analyses of 288 detrital zircons from three quartzite samples (LP11-03, CD10-10, and PIC-7). Greater than 98% of zircons are between 1400 Ma and 2000 Ma, and 99.6% of zircons have U/Th ratios <10, consistent with an igneous origin. Mesoproterozoic-age grains (ca. 1400 Ma) have especially low U/Th ratios.

ages in the same grain overlap within a  $\pm 10$  Ma uncertainty, showing no evidence of metamorphic overgrowths. Altogether, the uniformly low U/Th ratios, well-defined concentric zoning, and absence of metamorphic overgrowth domains confirm an igneous origin for all detrital zircon grains.

Quartzite sample LP11-03 was collected from the type locality Cerro de las Marquenas Formation, just south of the Plomo Fault. Isotopic analysis yields 93 concordant ages (Fig. 13), showing a broad 1651-2055 Ma Paleoproterozoic population with a peak age at 1697 Ma. Several successive age peaks occur at 1775, 1910, and 2050, and there is a minor Archean population 2584-2704 Ma. Four percent of the population is Mesoproterozoic (1459-1475 Ma) and defines a small peak at 1467 Ma which represents the maximum depositional age of the Marquenas Formation.

Vadito conglomerate (PIC-7) was collected about 2 km south of the type locality Marquenas Formation, and Vadito quartzite (CD10-10) was collected about 20 km to the east adjacent to the Picuris-Pecos fault from a unit originally mapped as the Marquenas Formation quartzite (Fig. 4). Ninety-five concordant ages in each sample (Fig. 13) yield age probability peaks characterized by a relatively identical narrow, Paleoproterozoic unimodal age distribution (1690-1777 Ma) and a peak mode of 1707 Ma (PIC-7), and 1713 Ma (CD10-10). There are no Mesoproterozoic or Archean zircon, with the exception of one 2557 Ma Archean grain in PIC-7.

Metamorphosed granite (PIC-11) was collected from the eastern Picuris Mountains, south of the Vadito quartzite (Fig. 4). Twenty-five concordant igneous zircon ages fall between 1662-1767 Ma, and define a mean age of  $1698.9 \pm 2.3$  Ma (Fig. 15).

### **Metamorphic Monazite Ages**

Two Vadito Group quartzite samples, CD10-10 (also included in detrital zircon analysis) and CD10-12 were chosen for electron microprobe analysis based on the size ( $>15 \mu\text{m}$ ), abundance, and representative compositional variation in metamorphic monazite grains. Monazite included in analyses range in size from  $10 \times 15$  to  $50 \times 40 \mu\text{m}$ . Average ages and elemental concentrations of Ca, Th, and Y are summarized in Table 3 for each core and rim domain of all analyzed grains.

### *Compositional domains*

X-ray compositional maps of monazite grains selected for analysis show two distinct chemical zones interpreted as core and rim domains based on elemental concentrations of Ca, Nd, Th, U, and Y (Figs. 16, 17, 18, and 19). In sample CD10-10 core domains are defined by low elemental concentrations of Ca (0.39 wt %), Th (1.46 wt%), and Y (0.67 wt%). Rim domains are defined by higher elemental concentrations of Ca (0.44 wt%), Th (1.98 wt%), and Y (1.06 wt%). Grains have fairly uniform composition with respect to Nd and U. Chemical zoning in sample CD10-12 is characterized by a high Th (1.52 wt%) and Ca (0.52 wt%) core that decreases slightly along the rims (0.88 wt% Th and 0.45 wt% Ca). Zoning is flat with respect to Nd and Y,

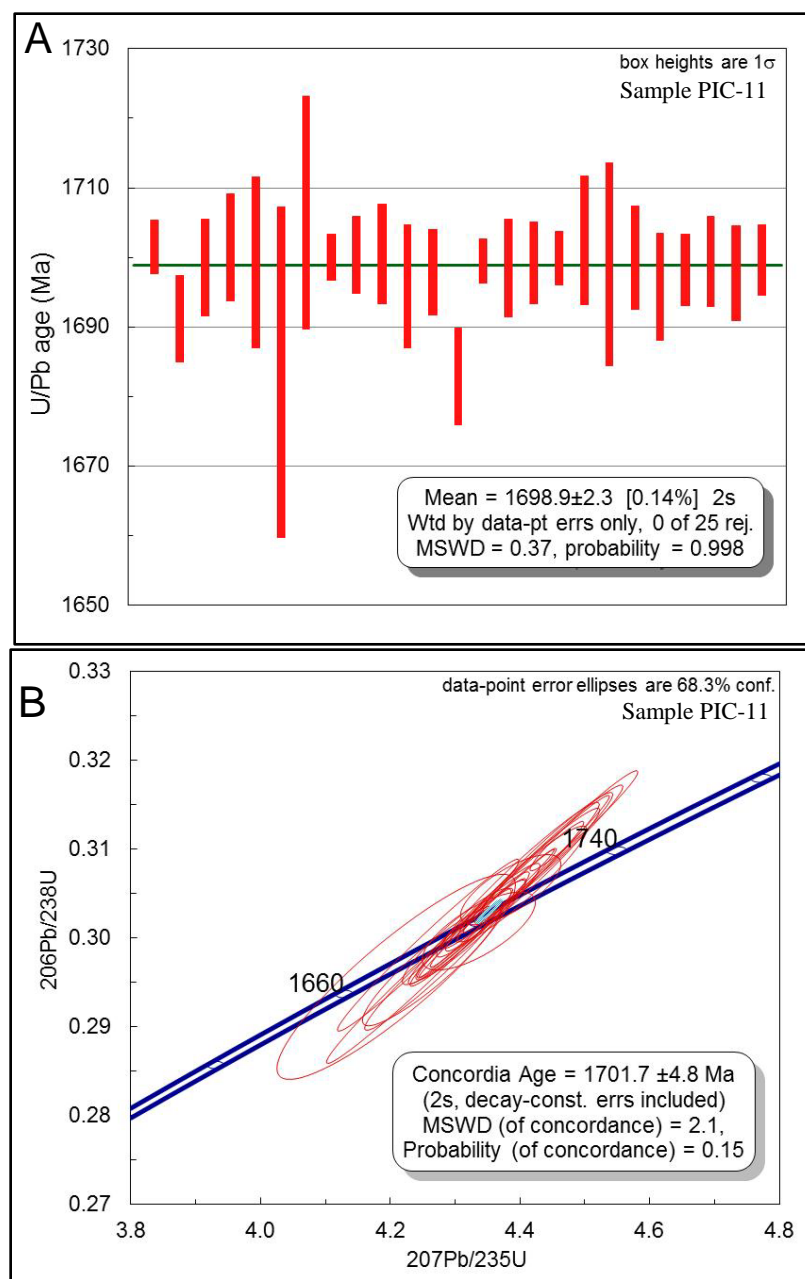


**Figure 15.** Average age histogram (A) and concordia diagram (B) of 25 igneous zircon grains from the Vadito Group Paleoproterozoic granitoid (PIC-11) collected from southeastern Picuris Mountains. Horizontal line in age plot indicates the mean age to be  $1699 \pm 2$  Ma and concordia diagram shows an average age of  $1702 \pm 5$  Ma.

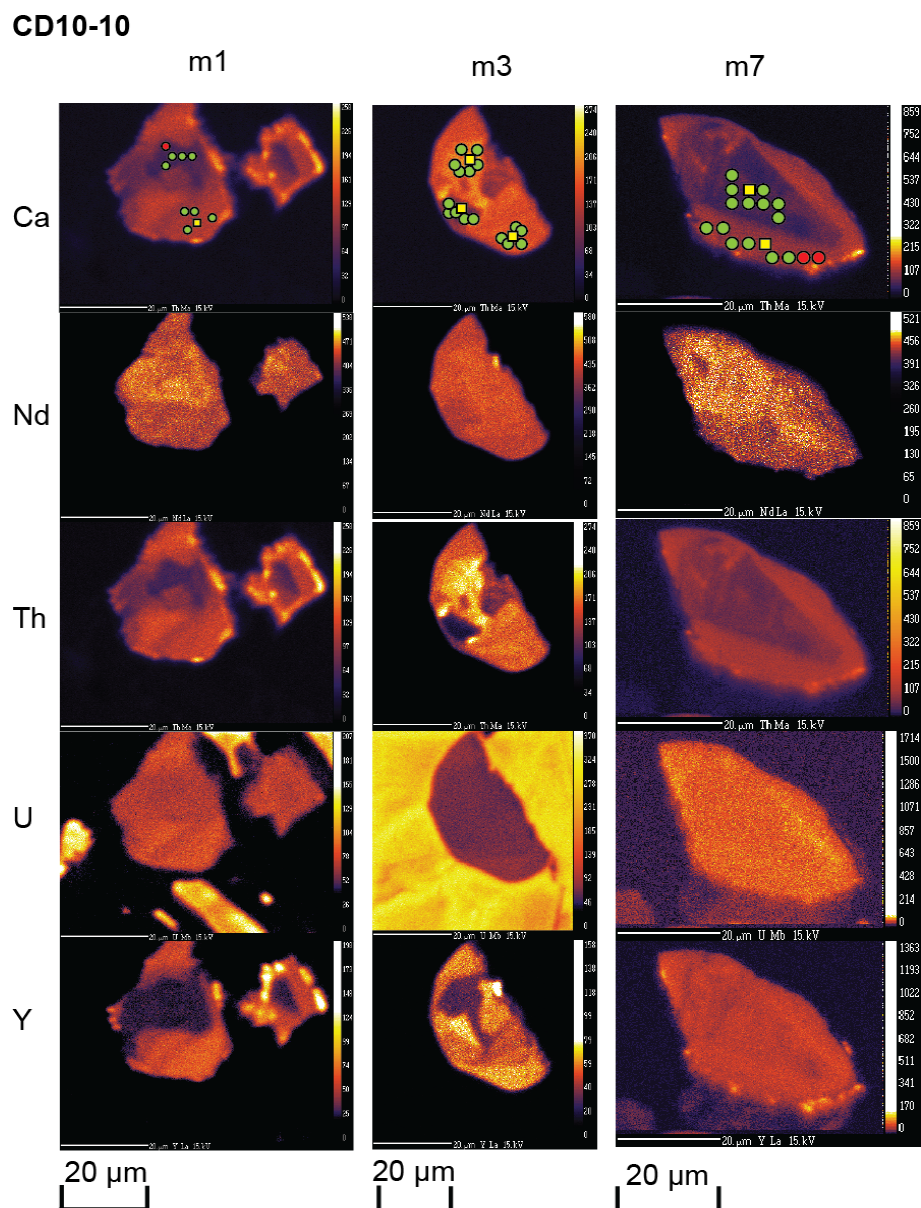


**Table 3.** Ages and compositional domains in monazites from samples CD10-10 and CD10-12.

<b>CD10-10</b>	<b>Age (Ma)</b>	<b>Ca</b>	<b>Th</b>	<b>Y</b>	<b>CD10-10</b>	<b>Age (Ma)</b>	<b>Ca</b>	<b>Th</b>	<b>Y</b>
m1 core	1510 ± 72	0.46	0.71	0.38	m1 rim	1389 ± 24	0.42	1.73	1.14
m3 core1	1418 ± 16	0.29	3.11	0.50	m3 rim	1385 ± 20	0.54	2.51	1.08
m3 core2	1563 ± 36	0.58	1.17	0.93					
m7 core	1538 ± 44	0.21	0.86	0.87	m7 rim	1448 ± 26	0.36	1.70	0.98
<b>Average</b>	1507 ± 42	0.39	1.46	0.67	<b>Average</b>	1407 ± 23	0.44	1.98	1.06

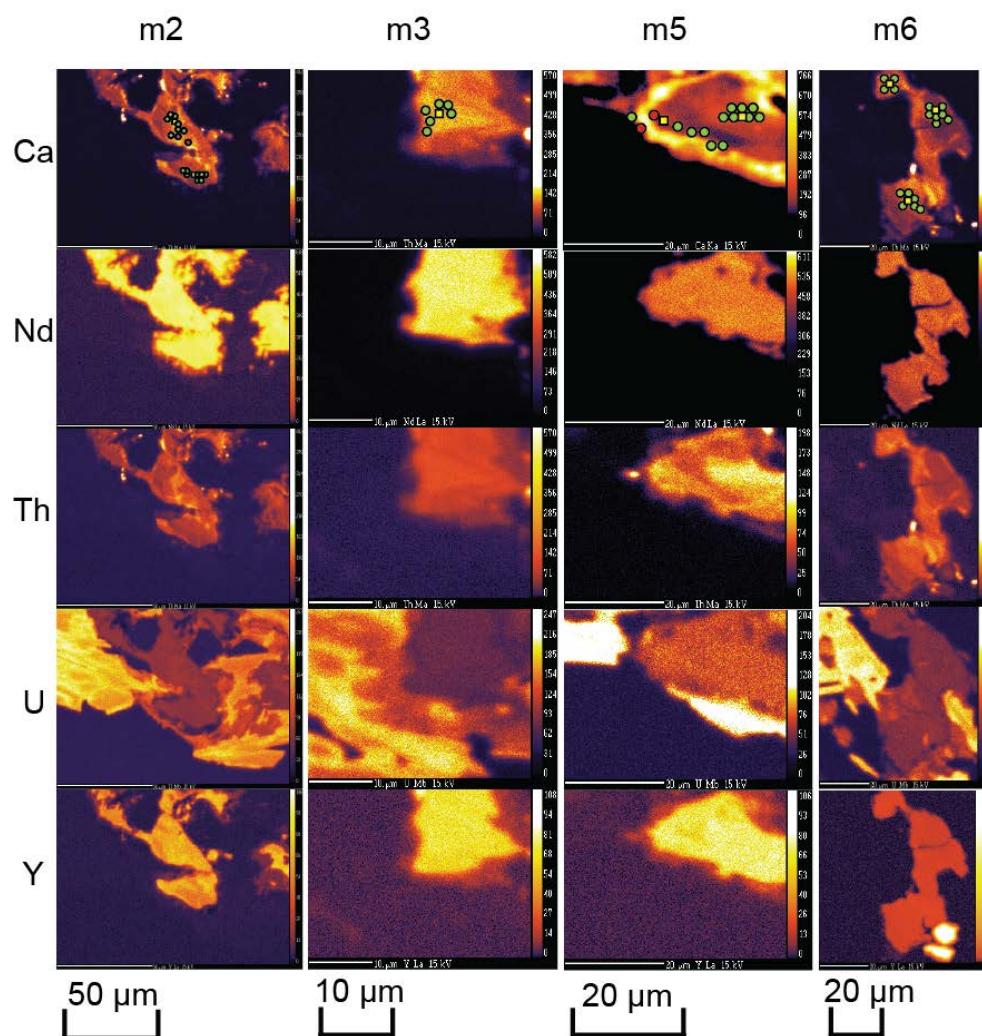
  

<b>CD10-12</b>	<b>Age (Ma)</b>	<b>Ca</b>	<b>Th</b>	<b>Y</b>	<b>CD10-12</b>	<b>Age (Ma)</b>	<b>Ca</b>	<b>Th</b>	<b>Y</b>
m2 core	1485 ± 24	0.54	1.58	1.18	m2 rim	1630 ± 50	0.52	0.82	0.82
m3 core	1432 ± 28	0.55	1.87	1.08					
m5 core	1409 ± 28	0.61	1.55	1.27	m5 rim	1452 ± 42	0.33	0.92	1.15
m6 core	1450 ± 40	0.36	1.09	1.14	m6 rim1	1485 ± 56	0.34	0.53	0.92
					m6 rim2	1470 ± 40	0.59	1.23	1.33
<b>Average</b>	1444 ± 30	0.52	1.52	1.17	<b>Average</b>	1469 ± 46	0.45	0.88	1.06



**Figure 16.** Composition maps of Th, Ca, Y, U, and Nd for three monazite grains from CD10-10 (m1, m3, m7). Warm colors (orange/yellow) indicate areas of high concentration. Cool colors (blue/purple) indicate areas of low concentration. Yellow points represent points where the background was measured, red points represent bad analyses, and green circles represent points of analysis clustered in separate domains defined by differences in concentration.

## CD10-12



**Figure 17.** Composition maps of Th, Ca, Y, U, and Nd for four monazite grains from CD10-12 (m2, m3, m5, m6). Warm colors (orange/yellow) indicate areas of high concentration. Cool colors (blue/purple) indicate areas of low concentration. Yellow points represent points where the background was measured, red points represent bad analyses, and green circles represent points of analysis clustered in separate domains defined by differences in concentration.

**Figure 18.** Elemental compositional maps of all monazite grains analyzed from samples CD10-10 and CD10-12 with respect to Y (A) and Ca (B). Recorded ages (Ma) of compositional domains are reported with standard error in respective domains of analysis. Warm colors (orange/yellow) indicate areas of high concentration. Cool colors (blue/purple) indicate areas of low concentration.

**Figure 18.**

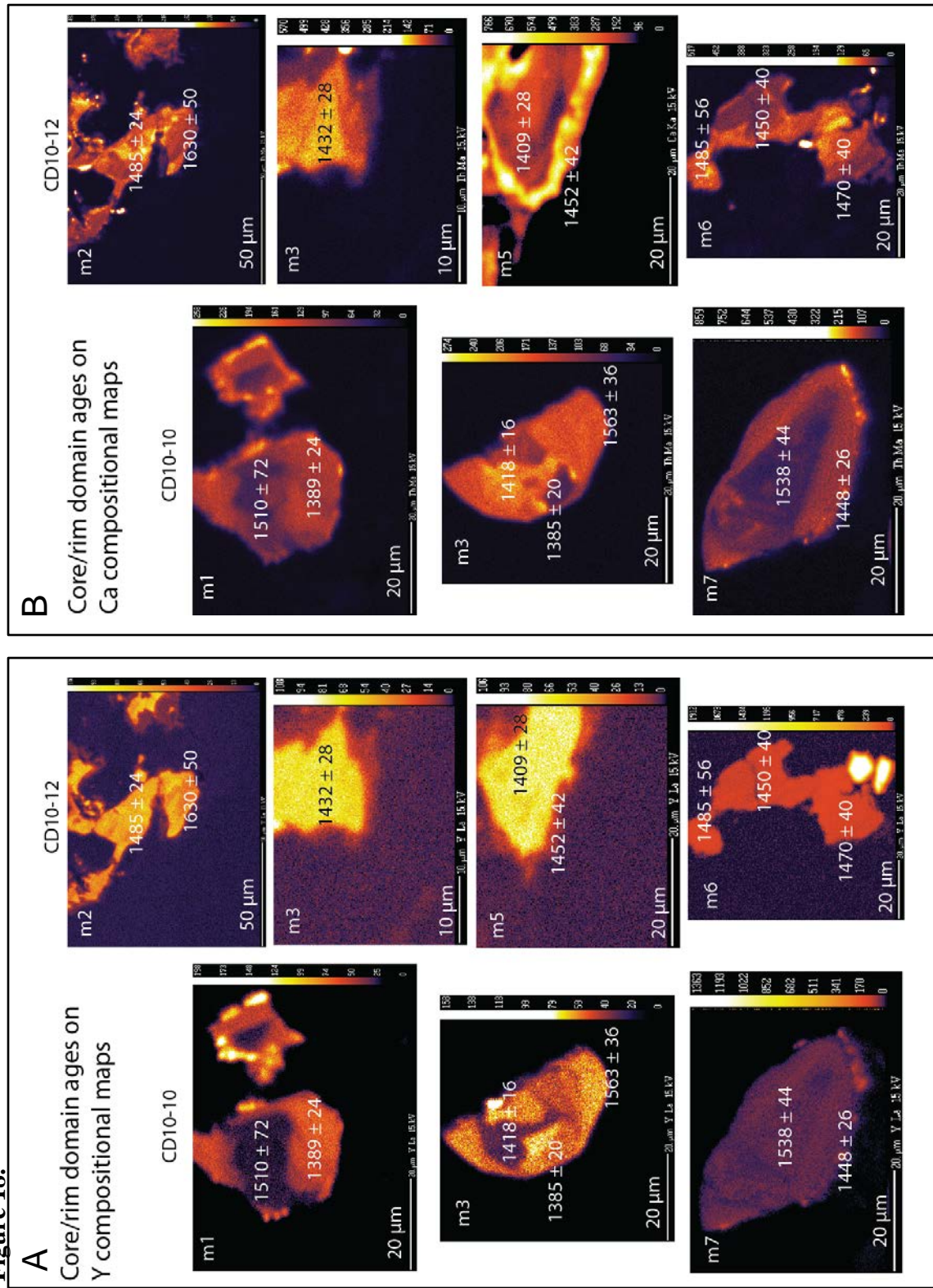
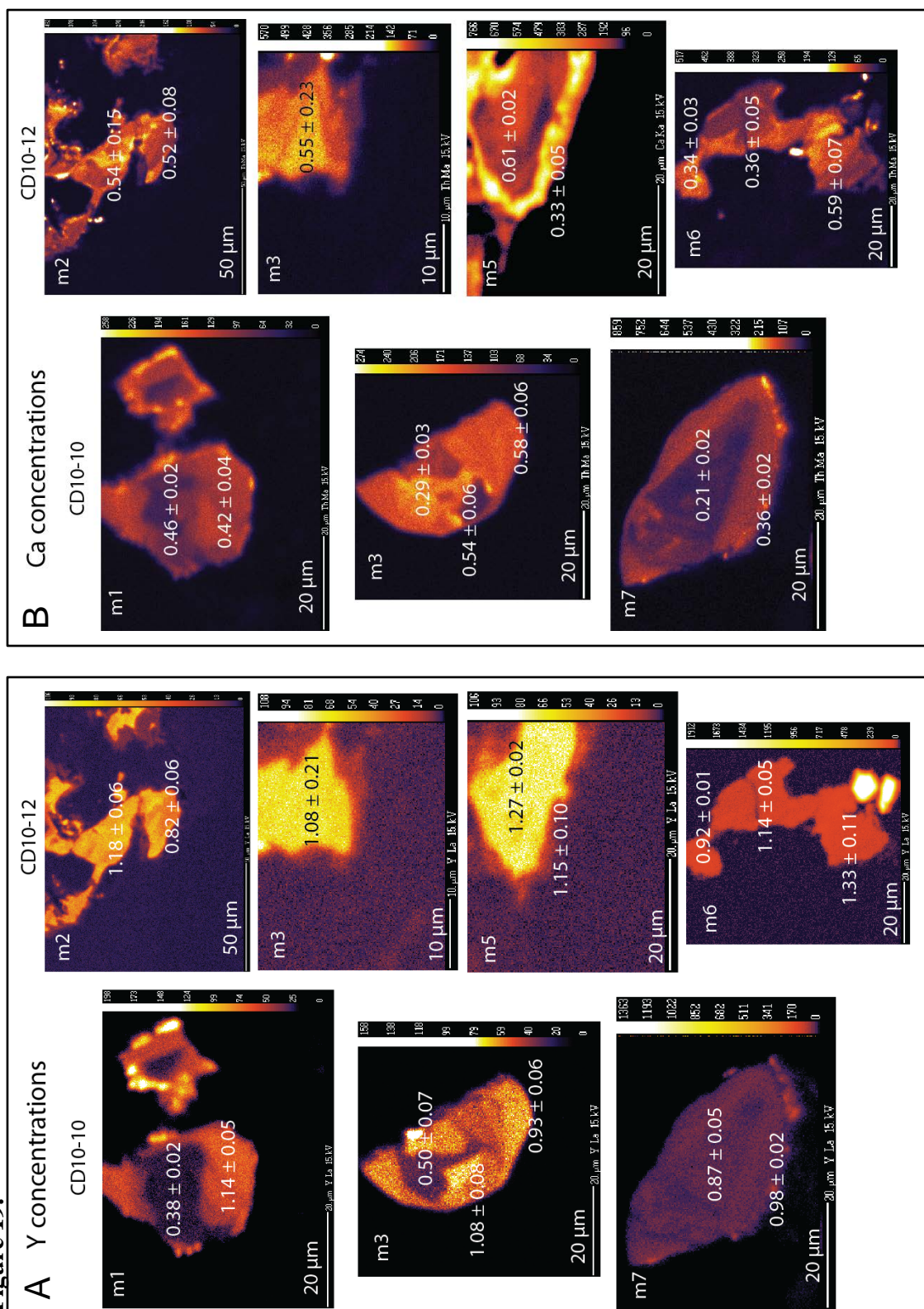


**Figure 19.** Elemental compositional maps of all monazite grains analyzed from samples CD10-10 and CD10-12 with respect to Y (A) and Ca (B). Warm colors (orange/yellow) indicate areas of high concentration. Cool colors (blue/purple) indicate areas of low concentration. Weight percent concentrations of the elements Y (A) and Ca (B) are calculated from a total average weight percent of 99.12 and are reported with a standard error in respective domains of analysis.

Figure 19.



and only minor chemical variation is present with respect to U. Grain m5 is unique, exhibiting an intermediate low concentration Th (0.33 wt%) and Ca mantle (0.92 wt%) between elevated Th (1.55 wt %) and Ca (0.61 wt%) core and rims (Fig. 19). Ages and chemical concentrations with respect to Th and Ca between core and rim domains in grain m6, are relatively consistent.

#### *U-Th-Pb chemical age data*

Domain ages (with  $2\sigma$  uncertainty) for both samples are reported in Fig. 20. Average core and rim ages from this study and from a previous study in the Picuris are plotted on a summary age histogram (Fig.21), and show dominantly Mesoproterozoic ages for metamorphic monazite growth. Three monazite grains in sample CD10-10 yield core ages from  $1418 \pm 16$  Ma to  $1563 \pm 36$  Ma, with an average age of  $1507 \pm 42$  Ma. Rim ages in the same sample range in age from  $1385 \pm 20$  Ma to  $1448 \pm 26$  Ma, averaging  $1407 \pm 23$  Ma. Four monazite grains in sample CD10-12 yield core ages from  $1409 \pm 28$  Ma to  $1485 \pm 24$  Ma, with an average of  $1444 \pm 30$  Ma. Rim ages in the same sample range in age from  $1452 \pm 42$  Ma to  $1485 \pm 56$  Ma, averaging  $1469 \pm 46$  Ma. Core and rim ages in each grain overlap within  $\pm 50$  Ma. Grain m2 (sample CD10-12) yields a single age of  $1630 \pm 50$  Ma. This domain is compositionally similar with respect to Y and Ca compared with other core and rim domains in the same sample, so it is difficult to assign it as a core or a rim. This 1.63 Ga age and ca. 1.5 Ga ages (sample CD10-10) are difficult to interpret, and are omitted from average age calculations (Fig. 21).



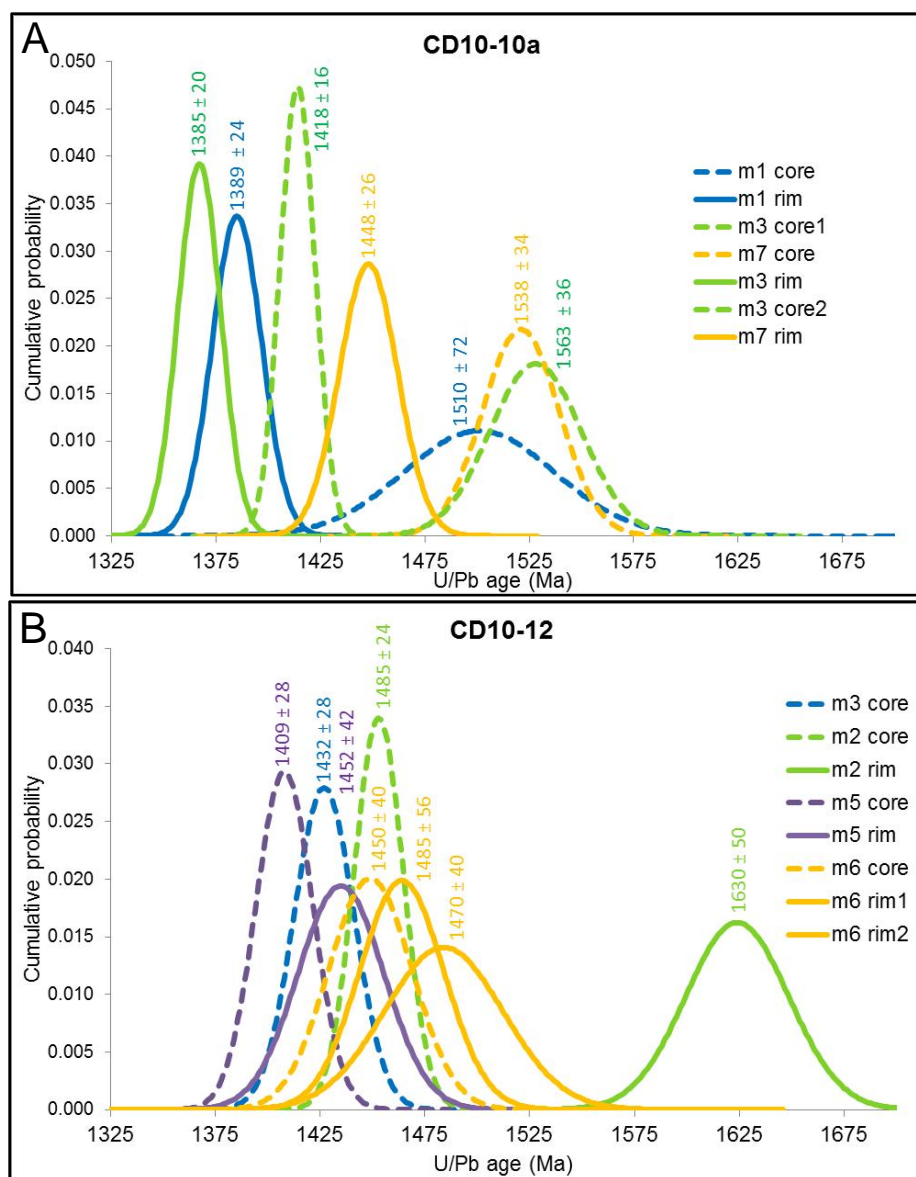


**Figure 20.** Age histograms showing all monazite domains analyzed. Mean, weighted mean, and  $2\sigma$  error for each set of analyses are represented by a normal probability Gaussian bell curve. Core domains are shown with a dashed line, and rim domains with a solid line. Sample CD10-10 (A) shows monazite ages from 3 grains and sample CD10-12 (B) shows monazite ages from 4 grains.

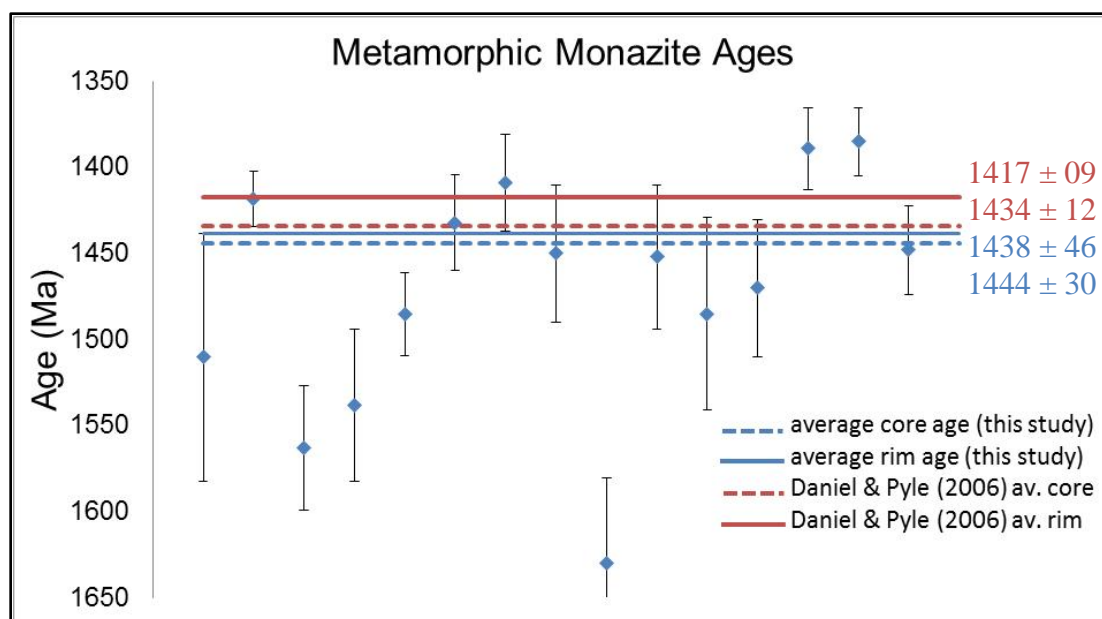


**Figure 21.** Age plot of all monazite ages recorded in this study (CD10-10 and CD10-12 in blue) as well as metamorphic monazite ages recorded in a previous study by Daniel & Pyle (2006) in red. Each data point represents the reported age for a single age domain within a monazite grain (core or rim) with  $2\sigma$  error. The mean core ages (dotted line) and mean rim ages (solid line) for all Mesoproterozoic ages in the region overlap within error, and range between 1417-1444 Ma. Older ca. 1.5 Ga ages and one 1.63 Ga age are also present, but these ages are difficult to interpret and are not included in the average.

## DISCUSSION

### Detrital zircon ages

The detrital zircon age spectrum for sample LP11-03 is nearly identical to the detrital zircon age spectra from samples PIC-2 and PIC-3 (Fig. 22) from Jones et al. (2011) for the same area. All samples show a broad 1.70-1.75 Ga Paleoproterozoic-age peak, as expected. However, 1.45-1.48 Ga Mesoproterozoic age peaks in three of the middle-to-upper Marquenas Formation quartzite samples (LP11-03, PIC-2, and PIC-3) represent the first evidence of Mesoproterozoic deposition in the southwest United States, and confirm the position of the Marquenas Formation as the youngest lithologic unit in the Picuris stratigraphic column (Fig. 6). All Mesoproterozoic detrital zircons from the Marquenas Formation, including my sample and those from Jones et al. (2011), are plotted in Figure 23, and record a maximum depositional age between 1.48-1.45 Ga.

Sampled from higher up in the stratigraphic section, PIC-3 records the youngest maximum depositional age (1.45 Ga), and contains the greatest amount and age range of Mesoproterozoic grains (27 grains between 1.42-1.48 Ga) as compared to the other two Marquenas samples (4-5 grains between 1.46-1.48 Ga in LP11-03 and PIC-2). This may be due to an increased amount of ca. 1.4 Ga material being deposited into the basin over time as the cratonic margin to the south of the Picuris continues to uplift.

Sample CD10-10 was collected about 20 km to the east of the type locality Marquenas Formation across discontinuous map units (Fig. 4) from a locality previously

mapped as the easternmost exposure of the Marquenas Formation. However, the detrital age distribution of CD10-10 lacks the Mesoproterozoic and Archean age peaks that are characteristic of other Marquenas Formation samples. The unimodal 1.71 Ga age peak in CD10-10 is nearly identical with the other Vadito Group sample (PIC-7). The unit was originally mapped by Bauer (1988) as Vadito Group quartzite with intruding 1.68 Ga granitoids, who describes the unit as “densely interlayered with amphibolites, felsites, and granitic rocks,” much different than the type locality Marquenas Formation quartzite to the west. Light microscope imaging shows that CD10-10 has a significant microcline component (Fig. 9), possibly derived from nearby “interlayered felsites and granitic rocks” in Vadito quartzite as described by Bauer (1988). Field observations from previous studies, closer mineralogical analyses, and detrital zircon ages suggest that the easternmost exposure of the Marquenas Formation (Fig. 4; as previously mapped) is not a stratigraphic equivalent to the Marquenas Formation. Instead, the sample location of CD10-10 would be better assigned as the Vadito quartzite.

Since the Kolmogorov-Smirnoff (K-S) statistical test determines the similarity of the detrital zircon age populations among samples, I included detrital zircon data from Jones et al., (2011) in the test in order to evaluate the correlation of age populations in all formations in the Picuris Mountains. Results of the K-S statistical test are summarized in Table 4. Sample CD10-10 has the highest similarity when compared to the other Vadito Group sample PIC-7 (.91). It also has high overlap and similarity with Marquenas Formation (.81) and Hondo Group (.78) samples. Relatively high P-values of sample CD10-10 compared to other formations do not necessarily correlate with an overlap in

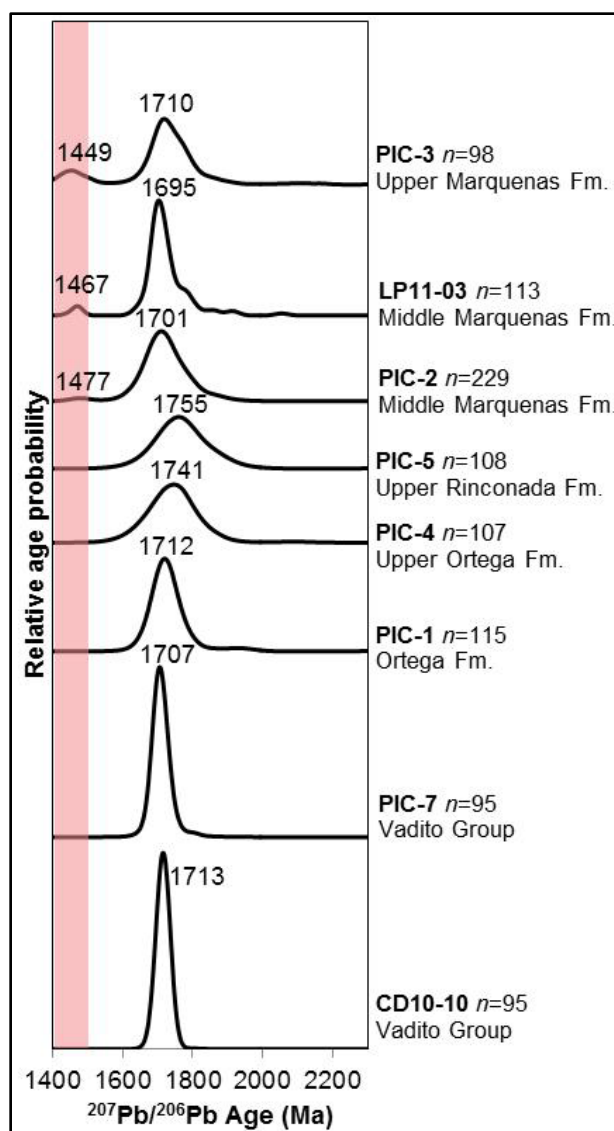


**Figure 22.** Normalized age probability plots showing distribution of U-Pb age determinations for 303 detrital zircon grains in my quartzite samples (LP11-03, CD10-10, and PIC-7) from the Vadito Group and Marquenas Fm, as well as 778 detrital zircon grains from five quartzite samples previously collected by Jones et al. (2011) from the Ortega Fm, Rinconada Fm, and Marquenas Fm. The red bar highlights the ca. 1480-1450 Ma timing of pluton activity in the regions; note correspondence to ca. 1.4 Ga age peaks in samples from the Marquenas Formation.

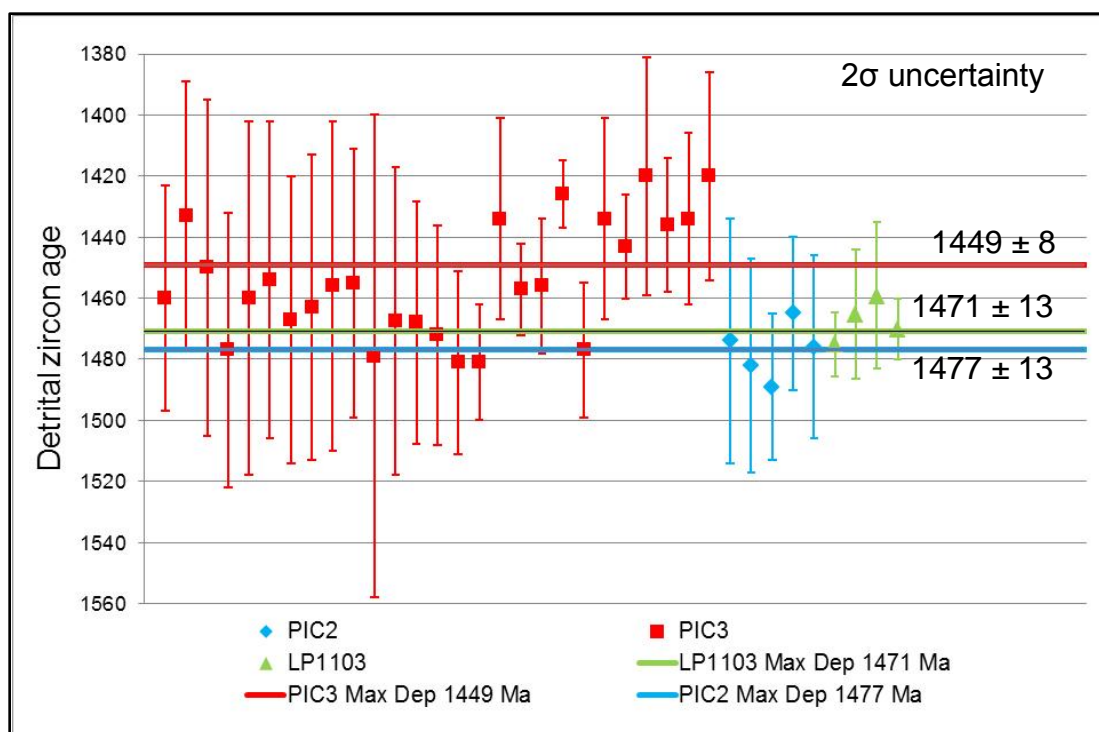


**Figure 23.** Average age plot of all Mesoproterozoic (ca. 1.4 Ga) detrital zircon grains from three quartzite samples from the middle to upper Marquenas Formation. Sample LP11-03 is in green; samples previously analyzed by Jones *et al.* (2011) are shown in blue (PIC-2) and red (PIC-3). Ages are in relative stratigraphic sequence from top to bottom. Each data point represents a spot analysis from individual zircon grains. Ages are calculated with 95% confidence and box heights are  $2\sigma$ . The horizontal lines indicate mean age of each sample. The mean ages of the youngest grain populations in each sample record the maximum depositional age. Maximum depositional ages for all samples overlap within error and average around 1.46 Ga.

**Table 4.** Results of the K-S statistical test

<b>K-S STATISTICAL TEST</b>								
<b>OVERLAP</b>								
	<b>CD10-10</b>							
<b>PIC-5</b>	0.297	<b>PIC-5</b>						
<b>PIC-1</b>	0.421	0.790	<b>PIC-1</b>					
<b>PIC-2</b>	0.309	0.852	0.681	<b>PIC-2</b>				
<b>PIC-3</b>	0.266	0.893	0.731	0.862	<b>PIC-3</b>			
<b>PIC-4</b>	0.279	0.863	0.743	0.790	0.915	<b>PIC-4</b>		
<b>PIC-5</b>	0.297	1.000	0.790	0.852	0.893	0.863	<b>PIC-5</b>	
<b>LP11-03</b>	0.637	0.524	0.505	0.563	0.495	0.515	0.524	<b>LP11-03</b>
<b>PIC-7</b>	0.577	0.601	0.680	0.622	0.550	0.553	0.379	0.674
<b>SIMILARITY</b>								
	<b>CD10-10</b>							
<b>PIC-5</b>	0.577	<b>PIC-5</b>						
<b>PIC-1</b>	0.783	0.853	<b>PIC-1</b>					
<b>PIC-2</b>	0.715	0.884	0.902	<b>PIC-2</b>				
<b>PIC-3</b>	0.674	0.848	0.857	0.898	<b>PIC-3</b>			
<b>PIC-4</b>	0.649	0.913	0.879	0.918	0.886	<b>PIC-4</b>		
<b>PIC-5</b>	0.577	0.955	0.853	0.884	0.848	0.913	<b>PIC-5</b>	
<b>LP11-03</b>	0.811	0.784	0.867	0.885	0.854	0.838	0.784	<b>LP11-03</b>
<b>PIC-7</b>	0.909	0.681	0.854	0.817	0.753	0.749	0.681	0.882

\*K-S overlap similarity program generated by the LaserChron lab, University of Arizona. Tables compare P-values to recognize similarity of age populations between all samples including my samples (CD10-10, PIC-7 and LP11-03) and samples previously analyzed by Jones et al. (2011) from the Picuris Mountains. All P-values are >.05 suggesting that no two samples are sourced from significantly different populations (Guynn, 2006, Gehrels, 2010).

age populations (Guynn, 2006, Gehrels, 2008), but the similarity of Marquenas Formation ages to the adjacent Vadito Group samples confirm that it is likely locally sourced by these older rocks.

### *Provenance of the Marquenas Formation*

Depositional ages recorded by detrital zircon, lithological descriptions, and paleocurrent data allow for interpretation about the depositional environments and provenance of the Marquenas Formation. This information is essential in understanding the regional tectonic history of north-central New Mexico in the Mesoproterozoic. Detrital zircon ages, unimodal north and bimodal northwest-southeast paleocurrent indicators in the Marquenas Formation (Fig. 24; Soegaard & Eriksson, 1986), mineralogical and textural observations of Marquenas conglomerate clasts (Mawer et al., 1990), and ages of exposed plutons and detrital grains from Vadito Group rocks to the south of the type locality Marquenas Formation (Figs. 25 and 26), help to determine provenance for the Marquenas Formation.

There are many possible sources for Paleoproterozoic detrital zircons (1780-1695 Ma) in the Marquenas Formation quartzite. The deformed granite (PIC-11) dated in this study records an age of 1.70 Ga (Fig. 15). The proximal location of this granite just south of the Vadito quartzite in the southern Picuris suggests that PIC-11 is a likely source for Paleoproterozoic ages in the Vadito quartzite samples (CD10-10 and PIC-7). Other likely sources are the 1765 Ma Pecos Complex, a plutonic succession associated with the Yavapai Orogeny in the Rincon Mountains to the south of the Picuris or other plutonic



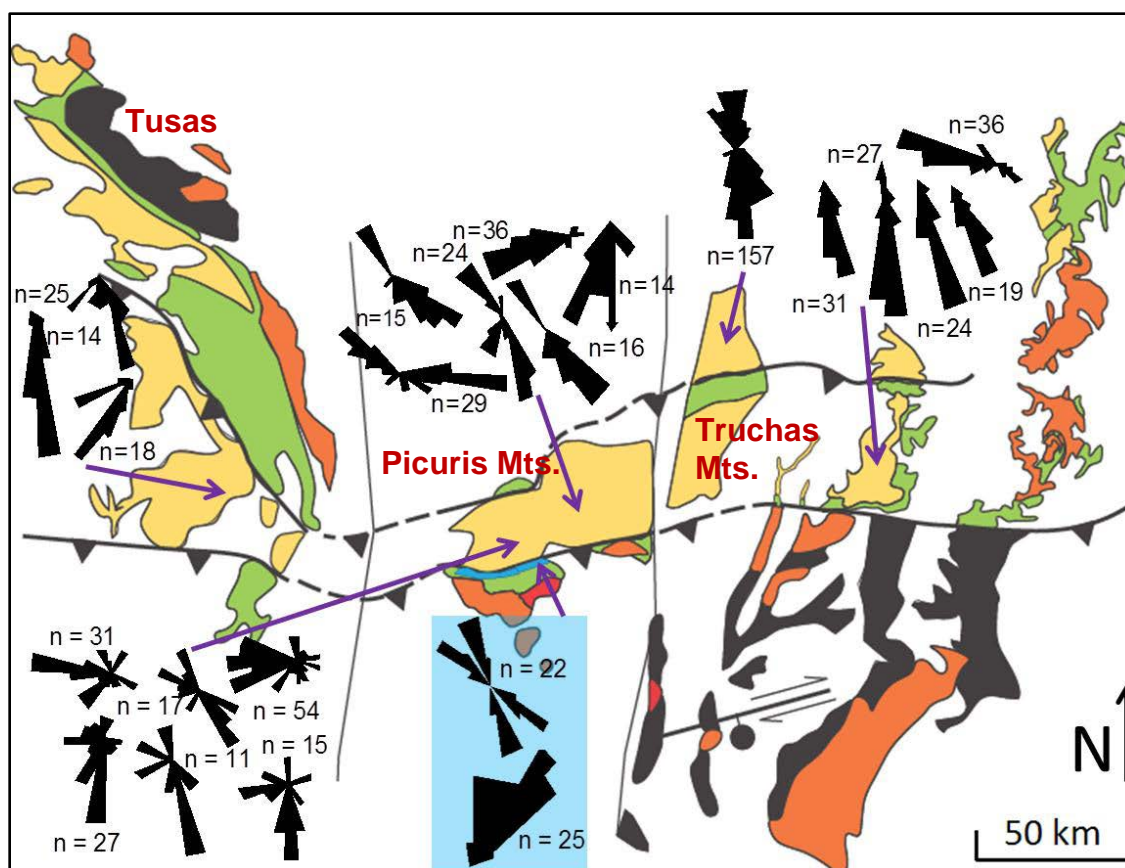


**Figure 24.** Reconstruction of Proterozoic rocks in northern New Mexico with a compilation of paleocurrent measurements from Barrett & Kirschner (1979) and Soegaard & Eriksson (1985, 1986). The Hondo Group is shown in yellow, Vadito Group in green, and Marquenias Formation in blue. Mesoproterozoic plutons are shown in red. Paleocurrent measurements from the Hondo Group indicate a south to bimodal NW/SE paleoflow. Paleocurrent data from the Marquenias Formation (highlighted in blue) shows a bimodal NW/SE and unimodal north-directed sediment transport.

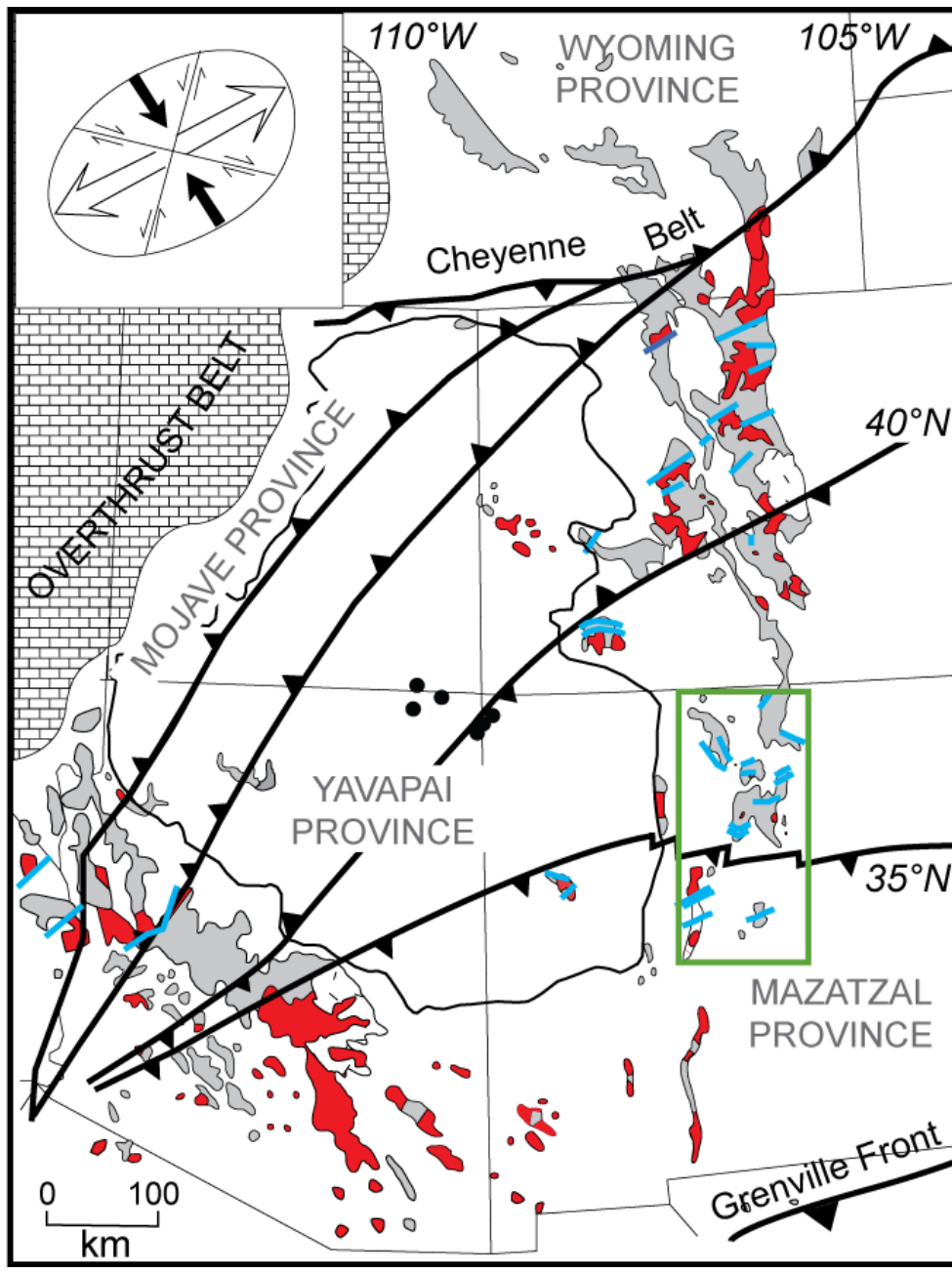


**Figure 25.** Regional map of the southwest U.S. showing Precambrian rocks in gray and the distribution of Mesoproterozoic (ca. 1.4 Ga) plutons in red. My study area in north central New Mexico lies within the green box (adapted from Jones et al., 2011).

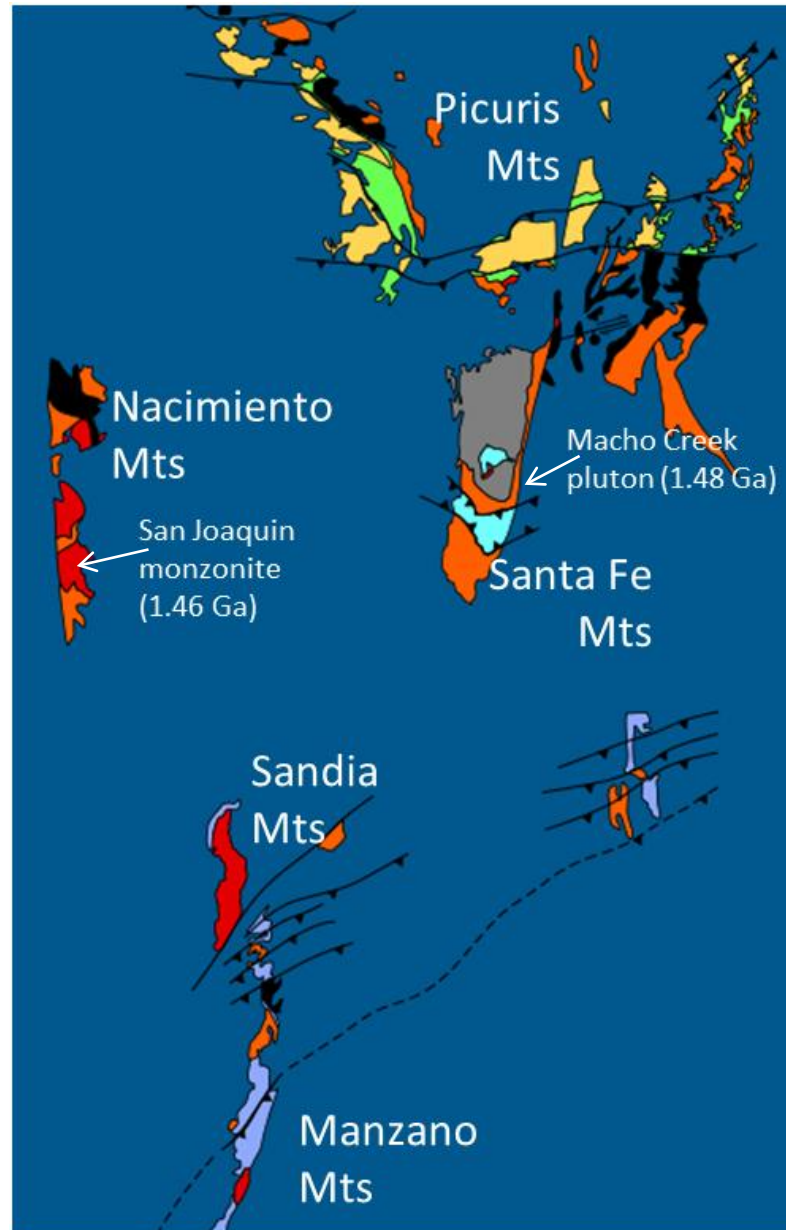


**Figure 26.** Reconstruction of Proterozoic Hondo and Vadito Group rocks in northern NM showing Mesoproterozoic plutons (red). The Macho Creek pluton (1.48 Ga) and San Joaquin monzonite (1.46 Ga) indicate possible sources of Mesoproterozoic detritus in the Marquenas Formation. This figure is modified from Karlstrom & Daniel (1993) and is the inset of the green rectangle in Figure 25.

successions to the north of the Picuris, such as the 1730 Ma Moppin and Gold Hill Complexes (Fig. 25; Jones et al., 2011; Karlstrom et al., 2004), Manzano Group volcanic and quartzite units (Jones et al., 2011), or 1730-1704 Ma volcanic-plutonic successions in southern Colorado and northern New Mexico (Jones et al., 2011; Bickford et al., 1989).

A normalized age probability plot (Fig. 22) shows peak Paleoproterozoic ages in the Marquenas Formation samples between 1701-1689 Ma. In comparison, Paleoproterozoic peaks in Vadito Group samples are 1710-1699 Ma, and in Hondo Group samples 1730-1718 Ma. Normalized data shows that Vadito Group Paleoproterozoic ages match the dominant peak in the Marquenas more closely than those in the Hondo Group, and together with sedimentological, textural, and mineralogical clast observations from previous studies (Mawer, 1990; Soegaard & Eriksson, 1986; Bauer, 1988), it is likely that the Marquenas is largely sourced from Vadito Group rocks. According to Mawer et al. (1990), mineralogical analyses of Marquenas clasts observe (1) no dispersed aluminum silicates which are dominant in the Hondo Group, (2) only 1% of clasts in the Marquenas are crossbedded- a prevalent feature in the Hondo Group quartzites, and (3) calc-silicate beds exposed in the Vadito section south of the Marquenas Formation (sample PIC-7) are mineralogically identical to pebbles in the lower Marquenas conglomerate. Additionally, porphyritic rhyolite pebbles with large phenocrysts and amphibolite pebbles are lithologically comparable to mafic and felsic components of the Vadito Group rocks (Soegaard & Eriksson, 1986). Consistencies in mineralogical composition, together with the dominance of Paleoproterozoic ages shown in detrital age distributions from

Marquenas Formation samples, strongly suggests locally sourced provenance of recycled Vadito Group metasedimentary and metavolcanic rocks.

Small populations of Archean grains (1.90 Ga, 2.05 Ga, 2.58 Ga, and 2.70 Ga) are present in the Marquenas detrital signature. These older grains are not present in surrounding Vadito Group or Hondo Group rocks (Fig. 13) and must be derived from other, possibly more distal, sources. Jones et al. (2011) propose that Archean grains in the Marquenas Formation were originally derived from the Trans-Hudson orogen and Black Hills to the north (Redden et al., 1990; Van Schmus et al., 1981) or the Grand Canyon and Mojave regions to the west (Fig. 25; Shufeldt et al., 2010; Hawkins et al., 1996; Wooden and DeWitt, 1991; Wooden et al., 1988).

Possible provenance for Mesoproterozoic detrital zircon ages (1.48-1.45 Ga) in the Marquenas Formation include: (1) rhyolites in the subsurface to the east that intrude the Vadito Group ranging in age between 1.48-1.38 Ga (Jones et al., 2011; Karlstrom et al., 2004; Reed et al., 1993; Bauer, 1993; Van Schmus & Bickford, 1981), or (2) the more recent idea that Mesoproterozoic grains could be derived from exotic source terranes such as Australia or eastern Antarctica (Doe et al., 2012). Although subsurface rhyolite ages match detrital ages and lithologies of rare clasts in the Marquenas conglomerate, there are no known evidence of exposed rhyolitic terranes nearby, making them difficult to confirm as a source for Mesoproterozoic grains. The ages of plutonic and volcanic sources, combined with north-directed paleoflow measurements from Soegaard & Eriksson (1986) and low U/Th ratios of detrital zircon grains, indicate an igneous source

south-southeast of the type locality Marquenas Formation. Figure 25 shows the distribution of Mesoproterozoic plutons in the southwest United States. The ca. 1.45 Ga Penasco granite in southern Picuris mark the northern-most lateral extent of Mesoproterozoic plutonism in the region (Bauer, 1993) up until mid-Colorado and there are no known ca. 1.45-1.40 plutons as far as ~150-200 km north of the Marquenas Formation into mid-Colorado (Fig. 25). Therefore, Mesoproterozoic grains in the Marquenas Formation were derived from sources to the south of the Picuris. The 1.44 Ga Penasco quartz monzonite in the southern Picuris and various 1.42-1.40 Ga plutons in the Sandia and Manzano Mountains (Karlstrom et al., 2004; Bauer, 1993; McCarty, 1983) are younger in age than the Mesoproterozoic grains in Marquenas Formation samples. However, the Macho Creek pluton (1.48 Ga) in the Santa Fe Mountains, the Mineral Hill pluton (1.46 Ga) in the San Andreas Mountains (Amato, 2007; Roths, 1991), and the San Joaquin monzonite (1.46 Ga) in the Nacimiento Mountains, all represent possible sources for the 1.48-1.45 Ga detrital zircons in the Marquenas Formation (Fig. 26).

Finally, 1600-1488 Ma detrital zircon ages in southern Arizona lead to an alternate hypothesis for exotic provenance for Mesoproterozoic sediment flux in the southwest U.S. (Doe et al., 2012). It is speculated that Australia assumed a position adjacent to western Laurentia around 1.5 Ga supplying sediment to New Mexico and Arizona during orogenesis. Australia is amongst scarce documentation of Mesoproterozoic zircon worldwide, with widespread magmatism and tectonism ca. 1.60-1.49 Ga. Antarctica also has evidence of Mesoproterozoic tectonism and magmatism and although not as complete and abundant as the record in Australia, it is another possible

exotic source. Either way, the 1.60-1.49 Ga Mesoproterozoic ages documented in these non-Laurentian terranes (Doe et al., 2012) are generally older than the Mesoproterozoic age peak (1.48-1.45 Ga) recorded in Marquenas Formation samples, and are not likely the primary source.

### **Timing of Metamorphism**

It is apparent that the metamorphic event recorded by monazite grains in this study was experienced regionally by northern New Mexico, including the Marquenas Formation. All formations in the Picuris range contain metamorphic mineral assemblages that indicate amphibolite-facies conditions; the Marquenas locally containing garnet, staurolite, biotite, chlorite, and amphibole (Jones et al., 2011; Soegaard & Eriksson, 1986). Williams et al. (1999) document ca. 1.4 Ga monazite ages from Paleoproterozoic Hondo and Vadito Group rocks, and monazite inclusions in andalusite porphyroblasts age 1.45 Ga. All studies done in the Picuris agree that the Marquenas Formation experienced the same regional scale folding as the Vadito and Hondo Groups, which prompted the growth of aluminosilicate minerals present in the Marquenas Formation (Jones et al., 2011; Williams et al., 1999; Bauer, 1993; Mawer et al., 1990; Holcombe & Callender, 1982; Nielson & Scott, 1979; Miller et al., 1963).

Two quartzite samples (CD10-10 and CD10-12) from the Vadito Group in the Picuris Mountains show monazite grains with Mesoproterozoic core and rim domains ranging from 1.56-1.44 Ga, and one 1.63 Ga age (Table 3). Observed compositional variation distinguishes the  $1630 \pm 50$  Ma domain (0.82 wt % Y) from other cores and

rims (1.17-1.06 wt % Y) in sample CD10-12. The Paleoproterozoic age corresponds closely with the Mazatzal orogeny, but its significance is unclear. It may represent lower temperature monazite growth possibly related to contact metamorphism in lower Vadito Group rocks caused by intruding ca. 1.69-1.65 Ga granitic plutons. Younger 1.49-1.45 Ga rims overgrow the 1630 Ma core, and are associated with 1.45-1.39 Ga regional metamorphism in northern New Mexico. Daniel & Pyle (2006) found only 1.45-1.44 monazite ages and no evidence of older 1.65-1.50 Ga ages related to Mazatzal-or-later metamorphism and deformation. Possible explanations for the absence of older grains include (1) missing older age domains during analysis, (2) older metamorphic monazite grains dissolved prior to or during ca. 1.4 Ga metamorphism or (3) these rocks experienced a single, regional metamorphic event at 1450-1435 Ma. In our study, the 1630 Ma age is not necessarily indicative of widespread, Mazatzal orogeny related metamorphism, but rather that it was a result of localized heating due to plutons.

The average core age of  $1507 \pm 42$  Ma recorded by monazite in sample CD10-10 is not representative of metamorphic monazite ages previously reported in northern New Mexico (Daniel & Pyle, 2006). The absence of pluton ages between 1.60-1.48 Ga document a magmatic gap period in southern Laurentia (Doe et al., 2012; Karlstrom et al., 2004). Therefore, the three monazite ages between 1563-1510 Ma recorded in sample CD10-10 could be a result of (1) lead loss in the isotopic system or (2) a mixing age due to a spot location with two overlapping domain ages. Unfortunately, concordance cannot be measured in monazite with microprobe chemical ages. However, lead loss in 1.65-1.60 Ga metamorphic monazite grains could cause younger, discordant ages and is a



plausible explanation for the 1.50 Ga cores. Alternatively, the microprobe electron beam might have overlapped a contact between an older ca. 1650-1600 Ma core and a younger 1450-1400 Ma rim, resulting in ca. 1550-1500 Ma mixed domain ages. Compositional variation (Fig. 16) shows a distinction between older core domains and younger rims, possible supporting evidence for this interpretation (0.91 wt % Th in 1.55-1.50 Ga cores and 2.26 wt % Th in 1.45-1.39 Ga rims). Acquiring isotope ratios of 1.56-1.50 Ga monazite ages in future studies would be helpful to test for concordance.

### **Regional tectonic implications**

The Marquenas Formation was deposited on a braided alluvial plain in response to a growing highland to the south, which may have formed in relation to movement along the Manzano thrust belt (Jones et al., 2011; Baer et al., 2003; Rogers, 2001). Dominantly quartzite and minor rhyolite clasts in the Marquenas conglomerate, together with north-northwest trending paleocurrent indicators (Soegaard & Eriksson, 1986), mineralogical analyses (Mawer et al., 1990), and overlap in dominant Paleoproterozoic detrital zircon age peaks, it is likely that the Marquenas Formation was derived from reworked local metasedimentary, metavolcanic, and igneous rocks including (1) Vadito Group rocks such as samples CD10-10 and PIC-7 in this study (2) the uplifted volcanic/sedimentary Manzano Group (Jones et al., 2011), (3) exposed Paleoproterozoic granites in the region such as PIC-11 in this study, (4) Mesoproterozoic-age granites south of the Picuris Mountains ca. 1.48-1.46 Ga, and (5) non-Laurentian source terranes

to the west-southwest that shed Mesoproterozoic sediment into the basin sometime before 1.45 Ga (Doe et al., 2012).

Findings in this study confirm evidence for regional orogenesis in the southwest U.S. between 1.47-1.44 Ga during a convergent or transpressional tectonic setting (Jones et al., 2011, 2010; Jessup et al., 2005; Shaw et al., 2001; Selverstone et al., 2000; Kirby et al., 1995; Nyman et al., 1994). South of the Picuris, the boundary that separates Yavapai and Mazatzal crustal provinces (Fig. 25) was the margin of the continent at 1.7 Ga before the Mazatzal orogeny. This area may be an inboard zone of weakness within the craton that was reactivated in the Mesoproterozoic, causing intracratonic 1.4 Ga metamorphism, deformation, and uplift across northern New Mexico and Arizona. Mesoproterozoic 1.48-1.45 Ga detritus shed into basins that formed north of the weak crustal zone such as those in the Picuris and in central Arizona (Doe et al., 2012). Alternatively, it is possible that the Mazatzal Province collided with southern Laurentia around 1.44 Ga, a time much later than previously thought, deforming the rocks in northern New Mexico in a regional accretionary orogenic event. Dominantly Mesoproterozoic metamorphic monazite ages recorded in north-central New Mexico from this study, and from Daniel & Pyle (2006), better support the later model of an accretionary orogenic event around 1.44 Ga (Fig. 21).

## CONCLUSION

Mesoproterozoic detrital zircon and metamorphic monazite ages require that deposition, deformation, and metamorphism in the Marquenas Formation are constrained to the interval between 1447-1407 Ma. North-trending paleocurrent data in cross-bedded quartzite and pebble-to-boulder conglomerate lithologies suggest that the Marquenas Formation was deposited in a braided alluvial plain environment in response to syn-tectonic uplift south of the Picuris Mountains. Existing mineralogical descriptions of Marquenas conglomerate clasts, together with the exact overlap in Paleoproterozoic detrital zircon age peaks in Marquenas and Vadito Group samples show that provenance for Paleoproterozoic and Archean detrital grains in the Marquenas include reworked quartzite/metavolcanic units such as the Vadito Group, the Manzano Group and ca. 1.75-1.70 Ga plutonic complexes. Mesoproterozoic detrital zircons 1.48-1.45 Ga are most likely derived from exposed plutons to the south of the Picuris including the Macho Creek pluton (1.48 Ga) in the Santa Fe Mountains, the Mineral Hill pluton (1.46 Ga) in the San Andreas Mountains (Amato, 2007; Roths, 1991), and the San Joaquin monzonite (1.46 Ga) in the Nacimiento Mountains (Karlstrom et al., 2004; Bauer, 1993; McCarty, 1983). Alternatively, Mesoproterozoic zircon may have been sourced from exotic provenance, as proposed by Doe et al. (2012) for central Arizona.

Metamorphic monazite data from the Vadito Group record the timing of metamorphism and deformation of Proterozoic rocks in northern New Mexico around 1444 Ma. Results of this study are consistent with a regional orogenesis in north-central

New Mexico between 1.45-1.40 Ga during a convergent or transpressional tectonic setting. It is possible that the Yavapai/Mazatzal boundary across northern New Mexico and central Arizona may have been reactivated in a Mesoproterozoic intracratonic orogenic event, uplifting and deforming the crust south of the Picuris, and accommodating sediment influx in new 1.48-1.45 Ga basins. Alternatively, the 1.65 Ga Mazatzal Province collided with the southern margin of Laurentia later than previously thought around 1.44 Ga, deforming the rocks in northern New Mexico in an accretionary orogenic event.

**REFERENCES**

- Amato, J.M., Heizler, M.T., Boullion, A.O., Sanders, A.E., Toro, J., McLemore, V.T., Andronicos, C.L., 2011, Syntectonic 1.46 Ga magmatism and rapid cooling of a gneiss dome in the southern Mazatzal Province: Burro Mountains, New Mexico: *Geological Society of America Bulletin*, v. 123, no. 9-10, p. 1720-1744.
- Baer, S.H., Karlstrom, K.E., Williams, M.L., Jercinovic, M.J., Rogers, S., and Schneeflock, F., 2003, Geometry and timing of movements in the Proterozoic Manzano thrust belt, central New Mexico: *Geological Society of America Abstracts with Programs*, v. 35, no. 5, p. 42.
- Barrett, M.E., and Kirschner, C.E., 1979, Depositional systems in the Rinconada Formation (Precambrian), Taos County, New Mexico: *New Mexico Geological Society Guidebook, 30th Field Conference, Santa Fe County*, p. 121-127.
- Bauer, P., 1988, Precambrian geology of the Picuris Mountain, north-central New Mexico: *New Mexico Bureau of Mines and Mineral Research Open File Report 325*, p. 260.
- Bauer, P., Williams, M., 1989, Stratigraphic nomenclature of Proterozoic rocks, northern New Mexico – revisions, redefinitions, and formalization. *New Mexico Geology*, v. 11, p. 45-52.
- Bauer, P., Williams, M., 1993, Proterozoic tectonic evolution of the Picuris Mountains, Northern New Mexico. *The Journal of Geology*, 101, p. 483-500.
- Bauer, P., Williams, M., 1994, The age of Proterozoic Orogenesis in New Mexico, USA. *Precambrian Research*, v. 67, p. 349-356.
- Bell, T.H., 1986, Foliation development and refraction in metamorphic rocks: reactivation of earlier foliations and decrenulation due to shifting patterns of deformation partitioning. *Journal of Metamorphic Geology*, v. 4, p. 421–444.
- Bickford, M.E., Shuster, R.D., and Boardman, S.J., 1989, U-Pb geochronology of the Proterozoic volcano-plutonic terrane in the Gunnison and Salida area, Colorado, in Grambling, J.A. and Tewksbury, B.J., eds., *Proterozoic geology of the southern Rocky Mountains: Boulder, Colorado, Geological Society of America Special Paper 235*, p. 33-48.

- Daniel, C.G., Karlstrom, K.E., Williams, M.L., and Pedrick, J.N., 1995, The reconstruction of a middle Proterozoic orogenic belt in north-central New Mexico, U.S.A: New Mexico Geological Society Guidebook v. 46, p. 193-200.
- Daniel, C. G., Pyle, J. M., 2006, Monazite–xenotime thermochronometry and  $\text{Al}_2\text{SiO}_5$  reaction textures in the Picuris Range, northern New Mexico, USA: New evidence for a 1450–1400 Ma orogenic event. *Journal of Petrology*, v. 47, p. 97-118.
- Doe, M.F., Jones, J.V. III, Karlstrom, K.E., Thrane, K., Frei, D., Gehrels, G., and Pecha, M., 2012, Basin formation near the end of the 1.60-1.45 Ga tectonic gap in southern Laurentia: Mesoproterozoic Hess Canyon Group of Arizona and implications for ca. 1.5 Ga supercontinental configurations. *Lithosphere*, v. 4, p. 77-88.
- Gehrels, G.E., Valencia, V., Pullen, A., 2006, Detrital zircon geochronology by Laser-Ablation Multicollector ICPMS at the Arizona LaserChron Center, in Loszewski, T., and Huff, W., eds., *Geochronology: Emerging Opportunities*, Paleontology Society Short Course: Paleontology Society Papers, v. 11, p. 10.
- Gehrels, G.E., Valencia, V.A., and Ruiz, J., 2008, Enhanced precision, accuracy, efficiency, and spatial resolution of U-Pb ages by laser ablation-multicollector-inductively coupled plasma-mass spectrometry. *Geochemistry, Geophysics, Geosystems*, v. 9, p. 115-150.
- Grambling, J.A., and Williams, M.L., 1985, The effects of  $\text{Fe}^{3+}$  and  $\text{Mn}^{3+}$  on aluminum silicate phase relations in north-central New Mexico. *Journal of Petrology*, v. 26, p. 324-352.
- Gratz, R., Heinrich, W., 1998, Monazite-xenotime thermometry. III. Experimental calibration of the partitioning of gadolinium between monazite and xenotime. *European Journal of Mineralogy*, v. 10, p. 579-588.
- Guynn, J., 2006, Comparison of detrital zircon age distributions using the K-S test: Arizona LaserChron Center, University of Arizona.
- Harley, S.L., and Kelly, N.M., 2007, Zircon: tiny but timely. *Elements*, v. 3, p. 13-18.
- Hawkins, D.P., Bowring, S.A., Ilg, B.R., Karlstrom, K.E., and Williams, M.L., 1996, U-Pb geochronologic constraints on the Paleoproterozoic crustal evolution of the Upper Granite Gorge, Grand Canyon, Arizona. *Geological Society of America Bulletin*, v. 108, p. 1167-1181.

- Holcombe, R.J., Callender, J.F., 1982, Structural analysis and stratigraphic problems of Precambrian rocks of the Picuris Range, New Mexico: Geological Society of America Bulletin, v. 93, p. 138–149.
- Jessup, M.J., Karlstrom, K.E., Connely, J., Williams, M., Livaccari, R., Tyson, A., and Rogets, S.A., 2005, Complex Proterozoic crustal assembly of southwestern North America in an arcuate subduction system: The Black Canyon of the Gunnison, southwestern Colorado, in Karlstrom, K.E., and Keller, G.R., eds., *The Rocky Mountain Region: An Evolving Lithosphere*. Washington D.C., American Geophysical Union Geophysical Monograph no. 154, p. 21-38.
- Jones, J.V. III, Siddoway, C.S., and Connely, J.N., 2010, Age implications of ca. 1.4 Ga deformation across a Proterozoic mid-crustal section, Wet Mountains, Colorado, USA. *Lithosphere*, v. 2, p. 119-135.
- Jones, J. V., Daniel, C. G., Frei, D., Thrane, K., 2011, Revised regional correlations and tectonic implications of Paleo- and Mesoproterozoic metasedimentary rocks in northern New Mexico, USA: New findings from detrital zircon studies of the Hondo Group, Vadito Group, and Marquenas Formation. *Geosphere*, v. 7, p. 974-991.
- Karlstrom, K. E., Bowring, S. A., 1988, Early Proterozoic assembly of tectonostratigraphic terranes in southwestern North America. *The Journal of Geology*, v. 96, p. 561-576.
- Karlstrom, K.E., Dallmeyer, R.D., and Grambling, J.A., 1997,  $^{40}\text{Ar}/^{39}\text{Ar}$  Evidence for 1.4 Ga Regional Metamorphism in New Mexico: Implications for Thermal Evolution of Lithosphere in the Southwestern USA. *The Journal of Geology*, v. 105, p. 205-224.
- Karlstrom, K.E., Humphreys, E.D., 1998, Influence of Proterozoic accretionary boundaries in the tectonic evolution of western North America: Interaction of cratonic grain and mantle modifications events: *Rocky Mountain Geology*, v. 33, p. 161-180.
- Karlstrom, K.E., Amato, J.M., Williams, M.L., Heizler, M., Shaw, C., Read, A., and Bauer, P., 2004, Proterozoic tectonic evolution of the New Mexico region: a synthesis, in Mack, G.H., and Giles, K.A., eds., *The Geology of New Mexico: a Geologic History* : Albuquerque, New Mexico, New Mexico Geological Society Special Publication no. 11, p. 1-34.
- Kirby, E., Karlstrom, K. E., 1995, Tectonic setting of the Sandia pluton; An orogenic 1.4 Ga granite in New Mexico. *Tectonics*, v. 14, p. 185-201.

- Ludwig, K.R., 2008, Isoplot 3.60. Berkeley Geochronology Center, Special Publication no. 4, p. 77.
- Mawer, C.K., Grambling, J.A., Williams, M.L., Bauer, P.W., and Robertson, J.M., 1990, The Relationship of the Proterozoic Hondo Group to Older Rocks, Southern Picuris Mountains and Adjacent Areas, Northern New Mexico, in Bauer, P.W., Lucas, S.G., Mawer, C.K., and McIntosh, W.C., eds., Tectonic Development of the Southern Sangre de Cristo Mountains, New Mexico: Socorro, New Mexico, New Mexico Geological Society Guidebook, 41<sup>st</sup> Field Conference, Sangre de Cristo Mountains, New Mexico p. 171-177.
- McCarty, R.M., 1983, Structural geology and petrology of part of the Vadito Group, Picuris Mountains, New Mexico [unpublished MS thesis]: Albuquerque, University of New Mexico, p. 159.
- Miller, J.P., Montgomery, A., Sutherland, P.K., 1963, Geology of part of the southern Sangre de Cristo Mountains, New Mexico: New Mexico Bureau of Mines and Mineral Resources Memoir v. 11, p. 106.
- Montel, J., Foret, S., 1996, Electron microprobe dating of monazite. *Chemical Geology*, v. 131, p. 37-53.
- Nielsen, K.C., Scott, T.E., 1979, Precambrian deformational history of the Picuris Mountains, New Mexico: New Mexico Geological Society Guidebook, v. 30, p. 113-120.
- Nyman, M. W., Karlstrom, K. E., Kirby, E., and Graubard, C.M., 1994, Mesoproterozoic contractional orogeny in western North America: Evidence from ca. 1.4 Ga plutons. *Geology*, v. 22, p. 901-904.
- Passchier, C.W., and Trouw, R.A.J., 2005, *Microtectonics: 2<sup>nd</sup>*, Revised and enlarged edition with 322 images.
- Read, A.S., Karlstrom, K.E., Grambling, J.A., Bowring, S.A., Heizler, M., and Daniel, C., 1999, A middle-crustal cross section from the Rincon Range, northern New Mexico: Evidence for 1.68-Ga, pluton influenced tectonism and 1.4-Ga regional metamorphism: *Rocky Mountain Geology*, v. 34, p. 67-91.
- Redden, J.A., Peterman, Z.E., Zartman, R.E., and DeWitt, E., 1990, U-Th-Pb geochronology and preliminary interpretation of Precambrian tectonic events in the Black Hills, South Dakota, in Lewry, J.F., and Stauffer, M.R., eds., *The Early Proterozoic Trans-Hudson Orogen of North America: Geological Association of Canada, Special Paper no. 37*, p. 229-251.



- Reed, J.C., Jr., Bickford, M.E., and Tweto, O., 1993, Proterozoic accretionary terranes of Colorado and southern Wyoming, in Reed, J.C., Jr., Bickford, M.E., Houston, R.S., Link, P.K., Rankin, D.W., Sims, P.K., and Van Shmus, W.R., eds., Precambrian: Conterminous U.S.: Boulder, Colorado, *Geological Society of America*, The Geology of North America, v. C-2, p. 110-121.
- Rogers, S.A., 2001, New structural interpretation, microstructural analysis, and preliminary monazite geochronology of Proterozoic rocks in the central Manzano Mountains, New Mexico [B.S. thesis]: Albuquerque, University of New Mexico, p. 25.
- Roths, P., 1991, Geology of Proterozoic outcrops in Dead Man and Little San Nicolas Canyons, southern San Andres Mountains, New Mexico: New Mexico Geological Society 42nd Field Conference Guidebook, p. 91–96.
- Silverstone, J., Hodgins, M., Aleinikoff, J.N., and Fanning, C.M., 2000, Mesoproterozoic reactivation of a Paleoproterozoic transcurrent boundary in the northern Colorado Front Range: Implications for ~1.7- and 1.4-Ga tectonism. *Rocky Mountain Geology*, v. 35, p. 139-162.
- Shaw, C.A., Karlstrom, K.E., Williams, M.L., Jercinovic, M.J., and McCoy, A.M., 2001, Electron-microprobe monazite dating of ca. 1.71-1.63 Ga and ca. 1.45-1.38 Ga deformation in the Homestake shear zone, Colorado: Origin and early evolution of a persistent intracontinental tectonic zone: *Geology*, v. 29, p. 739-742.
- Shaw, C.A., Heizler, M.T., and Karlstrom, K.E., 2005,  $^{40}\text{Ar}/^{39}\text{Ar}$  thermochronologic record of 1.45–1.35 Ga intracontinental tectonism in the southern Rocky Mountains: Interplay of conductive and advective heating with intracontinental deformation, in Karlstrom, K.E. and Keller, G.R., eds., *The Rocky Mountain region: An evolving lithosphere. Tectonics, geochemistry, and geophysics: American Geophysical Union Geophysical Monograph v. 154*, p. 163–184.
- Shufeldt, O.P., Karlstrom, K.E., Gehrels, G.E., and Howard, K.E., 2010, Archean detrital zircons in the Proterozoic Vishnu Schist of the Grand Canyon, Arizona: Implications for crustal architecture and Nuna supercontinent reconstructions. *Geology*, v. 38, p. 1099-1102.
- Soegaard, K., and Eriksson, K.A., 1989, Origin of thick, first-cycle quartz arenite successions: Evidence from the 1.7 Ga Ortega Group, northern New Mexico. *Precambrian Research*, v. 43, p. 129-141.
- Soegaard, K., and Eriksson, K.A., 1985, Evidence of tide, storm, and wave interaction on a Precambrian siliciclastic shelf; the 1,700 M.Y. Ortega Group, New Mexico. *Journal of Sedimentary Research*, v. 55, p. 672-684.

- Soegaard, K., and Eriksson, K.A., 1986, Transition from Arc Volcanism to Stable-Shelf and Subsequent Convergent-Margin Sedimentation in Northern New Mexico from 1.76 Ga. *The Journal of Geology*, v. 94, p. 47-66.
- Stacey, J.S., and Kramers, J.D., 1975, Approximation of terrestrial lead isotope evolution by a two stage model. *Earth and Planetary Science Letters*, v. 26, p. 207-221.
- Stacey, J.S., and Hedlund, D.C., 1983, Lead-isotopic compositions of diverse igneous rocks and ore deposits from southwestern New Mexico and their implications for early Proterozoic crustal evolution in the western United States. *Geological Society of America Bulletin*, v. 94, p. 43-57.
- Van Schmus, W.R., and Bickford, M.E., 1981, Proterozoic chronology and evolution of the midcontinent region, North America, in Kroner, A., ed., *Precambrian plate tectonics*. Amsterdam, Elsevier Publishing Company, p. 261-296.
- Williams, M.L., Jercinovic, M.J., and Terry, M.P., November, 1999, Age mapping and dating of monazite on the electron microprobe: Deconvoluting multistage tectonic histories. *Geology*, v. 27, p. 1023-1026.
- Williams, M. L., Jercinovic, M. J., 2007, *Electron imaging and compositional microanalysis: Monazite research at UMass*.
- Williams, M.L., 1991, Heterogeneous deformation in a ductile fold-thrust belt: The Proterozoic structural history of the Tusas Mountains, New Mexico. *Geological Society of America Bulletin*, v. 103, p. 171-188.
- Williams, M. L., Karlstrom, K. E., Lanzirotti, A., Read, A.S., Bishop, J.L., Lombardi, C.E., Pedrick, J.N., Wingstead, M.B., 1999, New Mexico middle-crustal cross sections: 1.65 Ga macroscopic geometry, 1.4 Ga thermal structure, and continued problems in understanding crustal evolution. *Rocky Mountain Geology*, v. 34, p. 53-66.
- Williams, M. L., 1982, *Geology of the copper occurrence at Copper Hill, Picuris Mountains, New Mexico*. [M.S. thesis], University of Arizona: Tucson, Arizona.
- Wooden, J.L., Stacey, J.S., Howard, K.A., Doe, B.R., Miller, D.M., 1988, Pb isotopic evidence for the formation of Proterozoic crust in the southwestern United States, in Ernst, W.G., *Metamorphism and crustal evolution of the western United States [Rubey Volume]*: Englewood Cliffs, New Jersey, Prentice-Hall, v. 7, p. 68-86.
- Wooden, J.L., DeWitt, E., 1991, Pb isotopic evidence for the boundary between the early Proterozoic Mojave and central Arizona crustal provinces in western Arizona, in

Karlstrom, K.E., ed., Proterozoic geology and ore deposits of Arizona: Tuscon, Arizona. Arizona Geological Society Digest, v. 19, p. 27-50.